慶應義塾大学経済学部研究プロジェクト

最終成果論文（2024 年度）

Taxonomy, phylogeny and physiological characteristics of the genus *Cryptomarasmius* (Agaricales) in Japan

経済学部 4 年　学籍番号：22102308

氏名：伊東永三郎

（指導教員：糟谷大河先生）

Index

1. Introduction

1.1. Background

Fungi are very important in that they intermediate between animals and plants. They decompose the remains of animals and plants such as animal dung, carcasses, leaf litter and decayed wood, and reduce them to inorganic nutrients for plants.

When fungi decompose leaf-litter, the succession of fungal flora is usually observed (Osono, 2018). Initially, sugar fungi dominant. As leaf sugars are depleted, fungi that decompose leaf cellulose become dominant. As leaf cellulose are depleted, fungi that decompose leaf lignin become dominant. After that, soil fungi that secondarily use decomposed products become dominant. Through these processes, plant leaves are decomposed and reduced to inorganic nutrients. These leaf-litter fungi contribute greatly to soil fertility. However, these fungi often have small-sized basidiomata, and are difficult to find in the field and identify so there are few studies of the diversity of these fungi.

Incidentally, some of these fungi have host specificity. Among them, some species of the genus *Cryptomarasmius* T.S. Jenkinson & Desjardin grow on fallen leaves or branches of specific host plant species. For example, *Cryptomarasmius corbariensis* (Roum.) T.S. Jenkinson & Desjardin is known to grow specifically on the leaves and branches of *Olea europaea* L. in Europe (Bozok et al., 2017). In Japan, *C. aucubae* (Neda) T.S. Jenkinson & Desjardin is known to grow specifically on the leaves and branches of *Aucuba japonica* Thunb. var. *japonica* (Neda and Doi, 1999). Recently, the unidentified species of *Cryptomarasmius* that grew specifically on the leaves of *Pittosporum tobira* (Thunb.) W.T. Aiton were also discovered in Japan (Kasuya et al., 2024). These fungi are easier to find and identify than other fungi that also have small-sized basidiomata because of their host specificity so species of the genus *Cryptomarasmius* are better suited to study their physiological characteristics such as the decomposition process and relationships with plants. However, in Japan, the known species of *Cryptomarasmius* are only *C. aucubae* (Neda and Doi, 1999) and *Cryptomarasmius* sp. tentatively reported on *P. tobira* (Kasuya et al., 2024). More diverse species of *Cryptomarasmius* having host specificity are reported outside Japan. Hence, in this study, the specimens that were tentatively treated as the member of *Cryptomarasmius* were collected from various plants in Japan. These specimens were collected on dead plant leaves, stems or aggregate follicles of *Hedera helix* L., *H. rhombea* (Miq.) Bean, *Ligustrum japonicum* Thunb., *L. lucidum* Aiton, *Magnolia grandiflora* L. and *O. europaea.*

Moreover, some species of *Cryptomarasmius* not only decompose litter, but also have pathogenicity to plants. Otsubo et al. (2011) reported that *C. aucubae* have pathogenicity to *A. japonica*. Therefore, other *Cryptomarasmius* species may also have potential ability as pathogens to these host plants. Host plants of fungi examined in the present study, i.e., *A. japonica*, *H. helix*, *H. rhombea*, *L. japonicum*, *L. lucidum*, *M. grandiflora*, *O. europaea* and *P. tobira* are widely distributed and cultivated in Japan. Hence, it is important for plant protection and cultivation to reveal physiological relationships between the species of *Cryptomarasmius* and host plants. However, the specimens newly collected in this study were different to the known Japanese species of *Cryptomarasmius* in their host plants and morphological characteristics. In other words, taxonomic and phylogenetic placements of these specimens are unclear. It is necessary to describe and classify the specimens to study their physiological characteristics.

For these reasons, this study investigates the diversity of *Cryptomarasmius* in Japan and conducts taxonomic examinations based on morphological characteristics of basidiomata and phylogenetic analyses using DNA sequence data. Furthermore, this study conducts culture experiments and inoculation tests, and discusses about the physiological characteristics and relationships between the species of *Cryptomarasmius* and their host plants.

1.2. Diversity of *Cryptomarasmius*

The genus *Cryptomarasmius* belongs to Basidiomycota, Agaricales, Physalacriaceae (Jenkinson et al., 2014). They are characterized by small-sized basidiomata (often less than 5cm), distant lamellae, wiry stipe and growing on dead plant bodies mainly in rain season and summer. In addition, some species of *Cryptomarasmius* have host specificity.

The species of *Cryptomarasmius* previously belonged to the section *Hygrometrici* Kühner (1933) of the genus *Marasmius* Fr. (Marasmiaceae). The species of sect. *Hygrometrici* was characterized by having a dark pileus formed by a hymeniform layer of broom cells, non-collariate lamellae and a wiry, dark insititious stipe (Jenkinson et al., 2014). After that, some researchers added some specimens in sect. *Hygrometrici* by their monological characteristics (Singer, 1976; Desjardin and Horak, 1997, Neda and Doi, 1998, Antonín, 2007).

The first phylogenetic analysis including the specimens in sect. *Hygrometrici* was conducted by Tan et al. (2009). They used four ITS sequence data obtained from *C. micraster* (Petch) T.S. Jenkinson & Desjardin (as then *M. micraster* Petch) and other specimens of *Marasmius*. In this analysis, the four specimens were placed within a single monophyletic clade, and this clade was sister group of the two clades containing several species of the sect. *Marasmius* subsect. *Sicciformes* Antonín. The clade of *M. micraster* was strongly supported by 100% ML bootstrap and 1.0 posterior probability. However, the clade including *M. micraster* and the sect. *Marasmius* subsect. *Sicciformes* was not supported by statistical support.

The second analysis was conducted by Antonin et al. (2012). They provided ITS and LSU sequence data of three specimens collected in Korea. For the results of phylogenetic analysis and morphological observations, they identify these specimens as *C. crescentiae* (Murrill) T.S. Jenkinson & Desjardin (then as *M. crescentiae* Murrill, the member of sect. *Higrometrici*).

The third phylogenetic analysis was conducted by Jenkinson et al. (2014). They included in this analysis, each five of ITS and LSU sequence data obtained from the specimens in sect. *Hygrometrici* of the genus of *Marasmius* such as *C. corbariensis*, *C. exustoides* (Desjardin & E. Horak) T.S. Jenkinson & Desjardin, *C. micraster*, *C. thwaitesii* (Berk. & Broome) T.S. Jenkinson & Desjardin (then as *M. corbariensis* Roum., *M. exustoides* Desjardin & E. Horak, *M. micraster*, *M. thwaitesii* Berk. & Broome) and *M. hudsonii* (Pers.) Fr. In this analysis, the four taxa in sect. *Higrometrici* (*M. corbariensis*, *M. exustoides*, *M. micraster*, *M. thwaitesii*) were placed within a clade with statistical support by 82% Bayesian posterior probabilities and 63% of ML bootstrap. This clade was not resolved as the sister group with the clade containing taxa of the genus *Marasmius* but was strongly supported as the sister with the clade containing the genera *Rhodotus* Maire, *Physalacria* Peck and *Cylindrobasidium* Jülich. In addition, Jenkinson et al. (2014) also conducted the constraint analysis enforcing the clade containing taxa of *Marasmius* sensu stricto and sect. *Hygrometrici*. In this analysis, all topologies were rejected because they are significantly ($P < 0.001$) less likely than the unconstrained ML topology. From these results, Jenkinson et al. (2014) transferred the members of the sect. *Hygrometrici* previously included in the genus *Marasmius* to the new genus *Cryptomarasmius*.

After the genus was established, many researchers reported specimens of *Cryptomarasmius* by phylogenetic analysis. Kiyashko et al. (2014) described *C. aucubae* firstly in Russia with ITS and LSU sequence data. They also showed by phylogenetic analysis that the specimens of *C. aucubae* from Russia and of *C. crescentiae* from Korea (Antonin et al., 2012) were placed within a same clade strongly supported by 100% ML bootstrap, 100% MP bootstrap and 1 Bayesian posterior probabilities. Furthermore, based on the result of morphological observations, they suggested that the morphological characteristics of *C. aucubae* is variable. Bozok et al. (2017) described *C. corbariensis* newly in Turkey with ITS sequence data. Dutta and Acharya (2018) described *C. exustoides* newly in India with ITS and LSU sequence data. Li and Bau (2024) described *C. aucubae* newly in China and described *C. changchunensis* T. Bau & S.Y. Li as a new species with ITS and LSU sequence data.

In Japan, *C. aucubae* is only known species of the genus described by Neda and Doi (1998). It is known to grow specifically on the dead leaves, stems and fruits of *A. japonica* in Japan. However, the specimens of *C. aucubae* from Russia (Kiyashko et al. 2014) grew on the dead leaves of *Phellodendron amurense* Rupr. var. *amurense* and other broadleaved trees. The specimens of *C. aucubae* from China (Li and Bau, 2024) grew on the dead leaves of *Quercus mongolica* Fisch. ex Ledeb. and *Ulmus pumila* L. According to the result of phylogenetic analysis, these specimens were placed within a same clade with the specimens of *C. aucubae* in Japan and it was strongly supported with 100% bootstrap and 1 Bayesian posterior probability (Li and Bau, 2024). From this result, it can be said that the relationships between *C. aucubae* and plants should be studied more.

Currently, a total of sixteen species of *Cryptomarasmius* were listed in the Index Fungorum (https://www.indexfungorum.org/names/names.asp, accessed at December 9, 2024). However, many species of the known *Cryptomarasmius* taxa have not been described with molecular phylogenetic studies. In addition, *C. aucubae* was reported to be probably pathogenic to *A. japonica* (Otsubo et al., 2011) but there are no further studies on physiological characteristics of *Cryptomarasmius*.

In this study, the fungal names and the taxonomical concepts of *Cryptomarasmius* and other taxa followed Index Fungorum, and those of the plant taxa followed Ylist (http://ylist.info/ylist_simple_search.html).

2. Taxonomic studies

2.1. Materials and methods

2.1.1. Preparations of specimens and culture strains

The specimens using in this study were collected from November 2023 to September 2024 from below sites in Japan (Table 1). Each specimen was photographed by camera in field and by camera with stereo microscope in the laboratory. All descriptions of macroscopic characters were obtained from fresh basidiomata. The following abbrevlations are applied to macroscopic descriptions: S = number of sulci of the pileus; L = number of lamellae reaching the stipe. Fresh basidiomata of each specimen were dried using freezer and silica gel. In addition to these specimens, some specimens and sequence data were provided by Dr. Taiga Kasuya and Mr. Shohei Wada who are the supervisor and supporter of this study (Table 1). Specimens examined in the present study were deposited at the mycological herbarium of the Department of Biology, Keio University.

Pileus of specimens were cut and soaked in DMSO buffer (Seutin et al. 1991) with the addition of 100 mM Tris-HCL (pH 8.0) and 0.1 M sodium sulfite (Na_2SO_3) for DNA extraction and then stored at 4 ℃, following the procedures of Hosaka (2009), Hosaka and Castellano (2008), and Hosaka et al. (2010).

Mycelial cultures of the specimens examined in this study were prepared using fallen spores. Water agar mediums in sterile petri dishes were prepared and a water agar block about 10 mm square was stuck to inside of the lid of these petri dishes. Pileus from the sample was cut into four equal parts by the sterilized surgical knife and fixed with the water ager block. If the pileus was too small to cut, the pileus was not cut and used as was. The dish was kept are at 25 °C out of direct sunlight. After 24 hours, basidiospores that fell down onto the agar surface from pileus and spore germinations were observed by microscopic examinations. In the laminar flow, germinated basidiospores were cut out with the agar piece by sterile surgical knife and transferred to a new PDA dish to grow. The dish was kept are at 25 °C out of direct sunlight (Table 1).

2.1.2. Light microscopy

For light microscopic observations, a small portion from the basidiomata were mounted in water, 3 or 5% (w/v) NH_4OH on glass slides; the samples were examined with a microscope ECLIPSE 80i (Nikon, Tokyo). More than 50 randomly selected basidiospores and elaters were measured by PhotoRuler version 1.1.3 (Onishi, 2010) with the photo taken under a light microscope at oil immersion (IMMERSION OIL TYPE F, Nikon, Tokyo) at 1,000X magnification. Basidiospores dimensions are reported as follows; (minimum–) average (–maximum) of length × (minimum–) average (–maximum) of width; Q, quotient of spore length and spore width in face view.

2.1.3. DNA extraction from basidiomata

Fungal DNA was extracted from the tissue fragments stored in DMSO buffer as previously mentioned.

DNA extractions from the tissue fragments used the modified CTAB extraction followed by glass milk purification methods as summarized by Hosaka (2009) and Hosaka and Castellano (2008). Briefly, samples were ground in liquid nitrogen using mortar and pestle. After grounding, samples were transferred to a tube containing 1 ml of 2X CTAB buffer and incubated at 65 °C for 1hour. Then, the tubes were centrifuged at 12000 rpm for 5 minutes and 500 ml of the supernatant was transferred into a new tube. 500 µl of chloroform: isoamyl alcohol (24:1) was added to remove proteins. The tubes were centrifuged at 12000 rpm for 5 minutes and 350 ml of the supernatant was transferred into a new tube. 1 ml of 6 M sodium iodine buffer (Hosaka and Castellano, 2008) (pH 6.8) was added and mixed for 1 hour to extract DNA. 25 µl of glass milk was added and the tubes were rotated for 1 hour at room temperature to adsorb DNA. The tubes were centrifuged at 12000 rpm for 5 seconds and the supernatant was removed. 500 ml of washing buffer (ethanol buffer) was added and the tubes were centrifuged at 12000 rpm for 5 seconds and the supernatant was removed. This washing step repeated twice. After finishing washing step, the tubes were centrifuged at 12000 rpm for 5 seconds and the remaining washing buffer were removed by pipette and dried by heating at 55 °C for 5 minutes. 120 µl of TE buffer were added in these tubes. Finally, the tubes were kept at room temperature for 10 minutes and centrifuged at 12000 rpm at 1 minutes and the supernatant was transferred into a new tube. DNA of the specimens were obtained by the above process.

DNA sequence data were obtained from internal transcribed spacer (ITS) and large subunit (LSU) of the nuclear rRNA. For amplifying ITS, the primer combination of ITS4 and ITS5 (White et al., 1990) was used. For amplifying LSU, the primer combination of LROR and LR5 (Vilgalys and Hester, 1990) was used. Polymerase chain reactions (PCR) were carried out using 20 µl reaction liquid containing 1µl of purified DNA, 0.5 µl of each primer, 10 µl of EME and 8 µl of purified water. Cycling parameters were 1 cycle of 94 °C for 3 minutes, 94 °C for 35 seconds, 51 °C for 30 seconds, 35 cycle of 72 °C for 1 minutes and 1 cycle of 72 °C of 10 minutes. PCR products were electrophoresed in 1.5% agarose gels, stained with cyber green and visualized under UV light and gene amplification was observed.

2.1.4. DNA extraction from the culture

Sequencing reactions were performed in a BioRad DNA Engine Dyad PTC-220 Peltier Thermal Cycler using the BigDye™ Terminator v3.1 Cycle Sequencing Kit (Thermo Fisher Scientific), according to manufacturer's instructions. Single-pass sequencing was performed on each template using universal primers. The fluorescent-labeled fragments were purified from the unincorporated terminators either by ethanol precipitation method or using the BigDye XTerminator™ Purification Kit (Thermo Fisher Scientific). The samples were analyzed by ABI 3730xl Analyzer (96 capillary type) (Thermo Fisher Scientific).

Table 1: Specimens using the present study.

Specimen No.	Locality	Host	Date	Collector
B3444	Ibaraki, Hitachiota, Shimomiyakawauchi	*Aucuba japonica* (leaf)	July 29, 2017	Taiga Kasuya
B3459	Ibaraki, Hitachiota, Shimomiyakawauchi	*Aucuba japonica* (leaf)	July 29, 2017	Taiga Kasuya
B4436	Ibaraki, Hitachiomiya, Morigane	*Aucuba japonica* (leaf)	September 1, 2021	Taiga Kasuya
B5198	Kanagawa, Miura, Hayama, Isshiki	*Aucuba japonica* (leaf)	April 4, 2024	Taiga Kasuya
B4675	Kanagawa, Yokohama, Kohoku, Hiyoshi, Hiyoshi Campus of Keio University	*Aucuba japonica* (leaf)	June 5, 2022	Taiga Kasuya
15	Tokyo, Minato, Mita, Mita Campus of Keio University	*Hedera helix* (leaf)	May 17, 2024	Eisaburo Ito
42	Kanagawa, Yokohama, Kohoku, Hiyoshi, Hiyoshi Campus of Keio University	*Hedera rhombea* (leaf)	July 2, 2024	Shohei Wada
B5142	Tokyo, Minato, Mita, Mita Campus of Keio University	*Ligustrum japonicum* (leaf)	November 17, 2023	Eisaburo Ito
B5148	Tokyo, Minato, Mita, Mita Campus of Keio University	*Ligustrum japonicum* (leaf)	December 13, 2023	Eisaburo Ito
B5265	Chiba, Ichikawa, Shinhama	*Ligustrum lucidum* (leaf)	June 29, 2024	Taiga Kasuya
B5205	Kanagawa, Yokohama, Kohoku, Hiyoshi, Hiyoshi Campus of Keio University	*Ligustrum lucidum* (leaf)	April 23, 2024	Eisaburo Ito
B5211	Tokyo, Minato, Mita, Mita Campus of Keio University	*Ligustrum lucidum* (leaf)	April 24, 2024	Eisaburo Ito
24	Tokyo, Minato, Mita, Mita Campus of Keio University	*Ligustrum lucidum* (leaf)	June 7, 2024	Eisaburo Ito
B5214	Tokyo, Minato, Mita, Mita Campus of Keio University	*Magnolia grandiflora* (aggregate follicles)	April 26, 2024	Eisaburo Ito
B5219	Tokyo, Minato, Mita, Mita Campus of Keio University	*Magnolia grandiflora* (aggregate follicles)	April 30, 2024	Eisaburo Ito

Table 1: continued.

Specimen No.	**Locality**	**Host**	**Date**	**Collector**
49	Tokyo, Minato, Mita, Mita Campus of Keio University	*Magnolia grandiflora* (aggregate follicles)	June 28, 2024	Eisaburo Ito
47	Tokyo, Minato, Mita, Mita Campus of Keio University	*Magnolia grandiflora* (leaf)	June 28, 2024	Eisaburo Ito
B5213	Tokyo, Minato, Mita, Mita Campus of Keio University	*Magnolia grandiflora* (leaf and branch)	April 24, 2024	Eisaburo Ito
B5218	Tokyo, Minato, Mita, Mita Campus of Keio University	*Hedera helix* (branch)	April 24, 2024	Eisaburo Ito
B5208	Kanagawa, Yokohama, Kohoku, Hiyoshi	*Olea europaea* (leaf)	April 23, 2024	Eisaburo Ito
B5212	Tokyo, Minato, Mita, Mita Campus of Keio University	*Olea europaea* (leaf)	April 24, 2024	Eisaburo Ito
B5000	Ibaraki, Kamisu, Hasaki	*Pittosporum tobira* (leaf)	July 18, 2023	Taiga Kasuya
B5070	Kanagawa, Chigasaki, Nanko, Nishihama	*Pittosporum tobira* (leaf)	October 9, 2023	Taiga Kasuya
B5442	Chiba, Choshi, Kimigahama	*Pittosporum tobira* (leaf)	October 18, 2024	Airi Urabe Eisaburo Ito Shohei Wada

2.1.5. Phylogenetic analyses

In this study, a total of 17 ITS and 15 LSU sequences were obtained, respectively. Thise sequences were assembled using ATGC ver. 6 (GENETYX, Tokyo). A total of 27 sequences from the GenBank were added to the analyses (Table 2; also see following). DNA sequences were aligned using Muscle ver. 3.6 (Edgar, 2004a; 2004b). The result of alignment was visually checked and corrected as necessary using BioEdit ver. 7.0.1 (Hall, 1999). Phylogenetic analyses by maximum likelihood and Bayesian methods were conducted with a combined dataset of above two loci. *Flammulina fennae* Bas (OM403362 of ITS and OM475610 of LSU) and *Rhodotus palmatus* (Bull.) Maire (MK287617 of ITS and MK287618 of LSU) were used as outgroup based on results presented by Jenkinson et al. (2014).

Maximum likelihood analyses were conducted using IQ-TREE version 2.2.2.6 for windows (Mihn et al., 2020). According to determine the lowest Bayesian information criterion scores (21386.003) by IQ-TREE the TN+F+I+G4 was chosen as the best-fit evolutional model for the analyses of the combined ITS and LSU dataset. Clade robustness were assessed by IQ-TREE using the Shimodaira-Hasegawa-like approximate likelihood ratio test (SH-aLRT; Guindon et al., 2010) and ultrafast bootstraps (UFBoot; Hoang et al., 2018) with 1000 replicates, respectively.

Bayesian analyses were conducted using MrBayes version 3.2.7 (Ronquist et al., 2012). The right substitution model (GTR+I+G) was selected as the combined dataset by hierarchical likelihood-ratio test using PAUP version 4.0b10 (Swofford, 2002) and MrModeltest2 (Nylander, 2004). The support of nodes was tested by posterior probabilities (PP).

Table 2: Sequence data obtained from the GenBank databases with these accession numbers. “n/a” means information not available.

Genus	**Species**	**Locality**	**Voucher**	**ITS**	**LSU**
Cryptomarasmius	*aucubae*	China, Jilin	HMJAU 68271	OR916265	OR915245
Cryptomarasmius	*aucubae*	China, Jilin	HMJAU 68272	OR916266	OR915246
Cryptomarasmius	*aucubae*	China, Jilin	HMJAU 68273	OR916267	OR915247
Cryptomarasmius	*aucubae*	Japan, Okinawa	435088	AB512314	AB512377
Cryptomarasmius	*celtibericus*	Bulgaria	SOMF30907	OR677893	n/a
Cryptomarasmius	*changchunensis*	China, Jilin	HMJAU 68269	OR916268sp	OR915248
Cryptomarasmius	*changchunensis*	China, Jilin	HMJAU 68270	OR916268sp	OR915248
Cryptomarasmius	*corbariensis*	USA, California	Ngyuen111209	JN601433	JN585128
Cryptomarasmius	*corbariensis*	Turkey, Osmaniye	FB00135	MF187561	n/a
Cryptomarasmius	*crescentiae*	Korea, Hongcheon	BRNM714783	JN003836	JN003842
Cryptomarasmius	*crescentiae*	Korea, Wonju	BRNM718790	JN003840	JN003845
Cryptomarasmius	*crescentiae*	Russia, Primorsky Krai	LE295992	KF774149	KF896252
Cryptomarasmius	*crescentiae*	Russia, Primorsky Krai	LE295993	KF774147	KF896251
Cryptomarasmius	*exustoides*	USA, Hawaii	DED6249	JN601434	JN585129
Cryptomarasmius	*exustoides*	India, West Bengal	AKD 209/2014	MF189078	MF495890
Cryptomarasmius	*micraster*	Malaysia, Pahang	TYS229	FJ431259	n/a

Table 2: continued.

Genus	Species	Locality	Voucher	ITS	LSU
Cryptomarasmius	*micraster*	Malaysia, Selangor	TYS237	FJ431260	n/a
Cryptomarasmius	*micraster*	Malaysia, Selangor	TYS391	FJ431258	n/a
Cryptomarasmius	*micraster*	Malaysia, Selangor	DED7647	FJ431261	n/a
Cryptomarasmius	aff *micraster*	New Zealand	PDD95297	KM975400	KM975386
Cryptomarasmius	*minutus*	Czech Republic	BRNM706959	KF774141	n/a
Cryptomarasmius	*thwaitesii*	China, Jilin	HMJAU68267	OR916270	OR915250
Cryptomarasmius	*thwaitesii*	China, Jilin	HMJAU68268	OR916271	OR915251
Cryptomarasmius	*thwaitesii*	USA, Hawaii	DED5918	JN601437	JN585132
Cryptomarasmius	*thwaitesii*	China	LF2131	MF769725	MF769726
Flammulina	*fennae*	Japan, Niigata	TNS F 82210	OM403362	OM475610
Rhodotus	*palmatus*	Germany	STMA14334	MK287617	MK287618

2.2. Results and discussions

2.2.1. Phylogenetic analyses

There was not major discrepancy among the result of maximum likelihood analyses and of Bayesian analyses so the discussion was conducted using the results of maximum likelihood analyses. The highest log likelihood of the result of maximum likelihood analyses was -10273.083. For Bayesian analyses, after 4650000 generation of Markov chain Monte Carlo runs, the analyses reached stationarity: the average standard deviation of split frequencies (ASDSF) dropped below 0.01 after 430000 generations.

For the results of phylogenetic analyses, all of the specimens of *Cryptomarasmius* were clustered within a strongly supported monophyletic clade [UFBoot (%)/SH-aLRT (%)/PP (%) = 100/99.8/100] (Fig. 1; also see following). A total of forty-nine taxa of the genus *Cryptomarasmius* constituted major monophyletic clade and they spread twenty clades in the major clade. The Japanese specimens examined in this study were placed within following four clades.

Clade 1 included the specimens 24, B5142, B5148, B5205, B5208, B5211, B5212 and B5265, collected on *L. japonicum*, *L. lucidum* and *O. europaea*. They were placed within a strongly supported clade [UFBoot (%)/SH-aLRT (%)/PP (%) = 99/98/100]. This clade was resolved as the sister with the clade containing *C. aucubae* (435088, B3444, B3459, B4436, B4675, B5198, HMJAU 68271, HMJAU 68272, HMJAU 68273, LE295992, LE295993) and *C. crescentiae* (BRNM714783, BRNM718790) with strong supports [UFBoot (%)/SH-aLRT (%)/PP (%) = 98/98.1/100]. The specimens B5208 and B5212 grew on the dead leaves of *O. europaea*. The specimen of *C. corbariensis* (FB00135) also grew on the dead branches and leaves of *O.*

europaea (Bozo et al., 2017) but the Japanese specimens and FB00135 were placed within different clades.

Clade 2 included the specimens B5213 and B5218, collected on fallen leaves and stems of *M. grandiflora* and fallen stems of *H. helix*. They were placed within a strongly supported clade with the specimens from China (HMJAU 68267 and HMJAU 68268) [UFBoot (%)/SH-aLRT (%)/PP (%) = 100/96.6/100]. This clade was the sister group with the clade containing *C. thwaitesii* (LE2131 and DED5918) with strongly supports [UFBoot (%)/SH-aLRT (%)/PP (%) = 100/100/100].

Clade 3 were included the specimens 49, B5214 and B5219, collected on fallen aggregate follicles of *M. grandiflora*. They were placed within a strongly supported clade with the specimens *C. exustoides* from India (AKD 209/2014) and from USA (DED6249) [UFBoot (%)/SH-aLRT (%)/PP (%) = 100/97.8/99.53].

Clade 4 were included the specimens 15, 42 and 47, collected on fallen leaves of *H. helix*, *H. rhombea* and *M. grandiflora*. They were placed within a strongly supported clade [UFBoot (%)/SH-aLRT (%)/PP (%) = 90/92.6/99.51]. This clade is the sister group with the clade containing the specimens *Cryptomarasmius* sp., collected on *P. tobira* from Japan (B5000, B5070 and B5442) with strong support [UFBoot (%)/SH-aLRT (%)/PP (%) = 90/91.6/99.21].

2.2.2. Morphological observations

For the results of morphological observations, the Japanese specimens using in this study could be distinguished into four types.

Type A included the specimens growing on fallen leaves of *L. japonicum* (B5142), *L. lucidum* (B5205, B5265) and *O. europaea* (B5212). They have dark brown, brown, light orange or light yellow pileus towards margin and sometimes yellowish-white or white at pileal margin, small-sized basidiospores (6.58-9.27 × 3.82-5.05 μm), developed caulocystidia and stipes covered spines on the top.

Type B included the specimens growing on fallen leaves of *H. helix* (15) and *M. grandiflora* (47). They had very small-sized basidiomata (pileus less than 1 mm, stipe 10 × 0.08 mm),narrow basidiospores (7.03-10.81 × 3.79-5.79 µm, Q = 1.89).

Type C included the specimens growing on fallen aggregate follicles of *M. grandiflora* (B5214 and 49). They have pileus colored dark brown or brown initially and white, pale yellow or brown towards margin, and thicker basidiospores (7.80-10.59 × 4.48-5.80 µm, Q = 1.74).

Type D included the specimens growing on fallen leaves and stems of *M. grandiflora* (B5213) and fallen stems of *H. helix* (B5218). They had pileus with hairs and developed sulci, colored dark brown or black initially and brown to dark brown towards margin, thicker stipe (1 mm), thick basidiospores (6.97-9.18 × 4.36-5.81 µm, Q = 1.62), and a hymeniderm pileipellis formed chains-like structure.

2.2.3. Comparison with phylogenetic analyses and morphological observations

Comparing the results of phylogenetic analyses and morphological observations, type A, type B, type C and type D detected by morphologies correspond Clade 1, Clade 4, Clade 3 and Clade 2, respectively. Each of these four morphological types were placed within a monophyletic group in the present phylogenetic analyses.

Phylogenetically, Clade 1 was close but distinct from the clade of *C. aucubae* and that of *C. changchunensis,* and these species morphologically different from the specimens of type A (Neda and Doi, 1998; Kiyashko et al., 2014; Li and Bau, 2024).

Clade 2 was phylogenetically close but distinct from the clade of *C. thwaitesii* (DED 5918 and LF 2131) and included the Chinese specimens of *C. thwaitesii* (HMJAU 68267 and HMJAU 68268). However, the specimens of type D were morphologically different from *C. thwaitesii* (Antonin, 2007; Puccinelli and Capelari, 2009).

Clade 3 was phylogenetically close but distinct from Clade 4 and the clade of *C. micraster* and *Cryptomarasmius* sp. from *P. tobira* in Japan (Kasuya et al., 2024) and these species ware morphologically different from the specimens of type C. Clade 3 includes *C. exustoides* and the morphological features of type C match with that of *C. exustoides* (Desjardin and Horak, 1997; Dutta and Acharya, 2018).

Clade 4 was phylogenetically close but clearly distinct from Clade 3 and *Cryptomarasmius* sp. from *P. tobira* in Japan (Kasuya et al., 2024) and these species morphologically different from the specimens of type B.

These Japanese specimens tentatively classified four morphological types and they were also distinct from other *Cryptomarasmius* species that were morphologically similar to them. The author therefore recognized the specimens of type A, type B and type D as new members of the genus *Cryptomarasmius* and type C as *C. exustoides,* previously not known in Japan. Detailed descriptions and illustrations of the salient features of the present new taxa and a newly recorded species are given below.

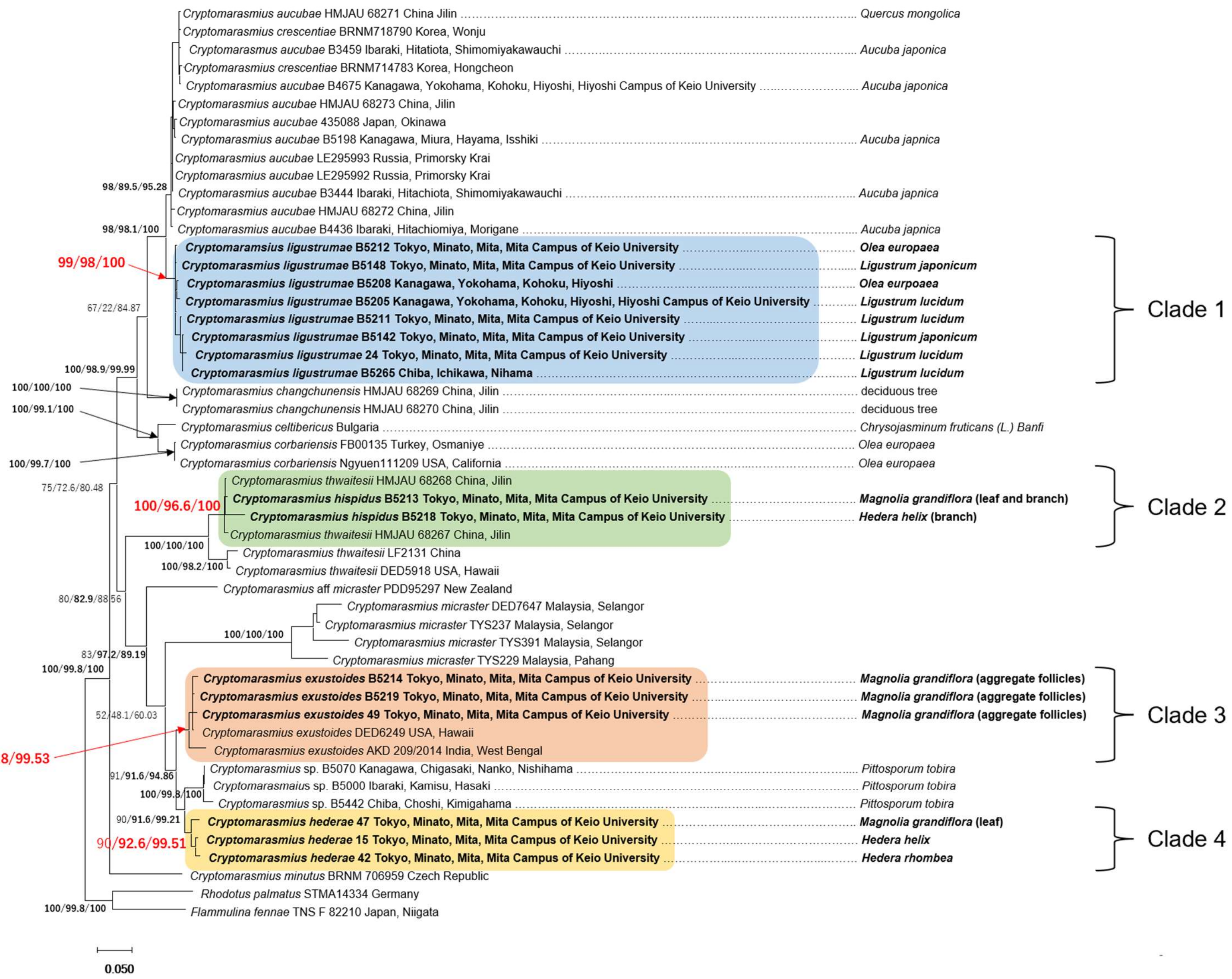

Fig. 1: Phylogenetic trees generated from maximum likelihood analysis. Major nodes supported by ≧95% UFBoot BS, 80% SH-aLRT BS and 90% Baysian PP. The numbers along branches are nodal supports (UFBoot/SH-aLRT/Bayesian PP). The potential host plant names are shown at the right side of the fungal specimen names, if they are identifiable

.

2.3. Taxonomy

Cryptomarasmius ligustrumae **E. Ito, sp. nov. (ad interim)**

Fig. 2

Pileus 2.0-3.0 mm broad, hemispherical or subconical when young, convex-expanded, slightly depressed when mature, shallow sulcate (S = 7-10), sometimes a little distorted, surface dry, glabrous, generally initially dark brown to brown overall, turns light orange or light yellow towards margin, sometimes yellowish-white or white at margin, rarely brown to dark brown overall, rarely initially dark reddish brown overall, turns reddish brown towards margin, brown or dark brown overall when dry, hygroscopic . Context very thin, cream. Lamellae 1 mm wide, white or translucent white, remote or adnexed, distant (L = 7-10) sometimes intervenose. Stipe 10-30 mm long, 0.15 mm wide, central, cylindrical, wiry, often tortuous but pileus upwards, equal, surface brown, dark brown or black overall, light orange or light yellow towards pileus, smooth, insititious. Rhizomorphs absent. Odor not distinctive.

Basidiospores (6.58–) 8.00 (–9.27) × (3.82–) 4.43 (–5.05) µm without germ pore, Q = 1.81, elongate, slightly curved toward germ pore, thin-walled, smooth, hyaline, amyloid. Pileipellis a hymeniderm, broom-cells of the Rotails-type, 11.9-23.6 × 8.4-14.4 µm, napiform to turbinate, pale brown, brown to dark brown on the top, achroic, pale yellow of pale brown on the bottom, spinose (spines < 1 µm) on the top, smoot on the bottom, thick-walled. Basidioles 16.5-21.1 × 4.37-6.21 µm, subulate to clavate, smooth, sometimes with papilla. Cheilocystidia of two types: a) 19.5-26.3 × 4.74-5.74µm; b). Caulocystidia 2.44-16.17 × 1.29-4.91 µm, subulate, sometimes capitate, smooth, hyaline. Stipe-derm spinose (spines < 1 µm) on the top.

Habit and Habitat: Solitary or gregarious on fallen leaves and branches of *L. lucidum*, *L. japonicum* and *O. europaea*, rarely on fallen leaves and branches of *A. japonica*. In planter, garden or mixed forest during all seasons, mostly rainy season and summer.

Holotype: JAPAN, Tokyo, Minato, Mita, Mita Campus of Keio University, scattered on fallen leaves of *L. japonicum* in the garden, November 17, 2023, Eisaburo Ito (B5142).

Etymology: The epithet refers to the genus of the Japanese plant *L. japonicum*, the host plant of the new species.

Additional specimens examined: Japan: Tokyo, Minato, Mita, Mita Campus of Keio University, fallen leaves of *L. lucidum* in the garden, April 24, 2024, Eisaburo Ito (B5211). Same place, fallen leaves of *L. lucidum* in the shrub of *A. japonica*, June 7, 2024, Eisaburo Ito (24). Same place, fallen leaves of *L. japonicum* in the garden, December 13, 2023, Eisaburo Ito (B5148). Same place, fallen leaves of *O. europaea* in the garden, April 24, 2024, Eisaburo Ito (B5212). Kanagawa, Yokohama, Kohoku, Hiyoshi, Hiyoshi Campus of Keio University, fallen leaves of *L. lucidum* in the mixed forest dominated by *L. lucidum* and *Q. serrata* Murray, April 23, Eisaburo Ito and Taiga Kasuya (B5205). Kanagawa, Yokohama, Kohoku, Hiyoshi, fallen leaves of *O. europaea* in the planter, April 23, 2024, Eisaburo Ito (B5208). Chiba, Ichikawa, Shinhama, fallen leaves of *L. lucidum* in the mixed forest dominated by *L. lucidum, P. tobira* and *Euonymus japonicus* Thunb., June 29, 2024, Taiga Kasuya (B5265).

Observations: *Cryptomarasmius ligustrumae* is characterized by small-sized pileus, brown to dark brown at the top of pileus and light orange or light yellow towards the pileal margin, yellowish-white or white at margin, distant lamellae (L = 7-10), the size of basidiospores 8.00 × 4.43 μm (without germ pores), the presence of caulocystidia, spinose stipe at the top. In addition, this species is characterized by its host plants, growing on fallen leaves of *L. japonicum*, *L. lucidum* and *O. europaea*.

Cryptomarasmius aucubae is phylogenetically close to *C. ligustrumae*. However, the two species ca be distinguished in that the size of the basidiospores of *C. aucubae* is narrower, 7-10 × 2.5-4.2 μm (Neda and Doi, 1999; Kiyashko et al., 2014; Li and Bau, 2024).

Cryptomarasmius changchunensis is also phylogenetically close to *C ligustrumae*. However, the two species can be distinguished that the color of the pileus of *C. changchunensis* is dark brown at center to brown at margin and the size of basidiospores of *C. changchunensis* is narrower (6.1-7.2 × 2.4-3.4 μm and Q = 2.10-2.77) (Li and Bau, 2024).

Cryptomarasmius corbariensis also grow on the leaves of *O. europaea*. However, the two species are distinguished in that *C. corbariensis* does not have caulocystidia whereas *C. ligustrumae* has them (Bozok, 2017).

Cryptomarasmius crescentiae is morphologically similar to *C. ligustrumae*. However, the two species are distinguished in that *C. crescentiae* has more dense lamellae (L = 7-18) (Desjardin and Horak, 1997) and smaller basidiospores (6.5 × 2.7 μm) (Kiyashko et al., 2014) than those of *C. ligustrumae*.

Cryptomarasmius minutus (Peck) T.S. Jenkinson & Desjardin is morphologically similar to *C. ligustrumae*. However, the present new species are distinguished from the former species in that the size of the basidiospores of *C. minutus* is smaller (6-8 × 2-4 μm; Kaplan et al., 2021) than those of *C. ligustrumae*.

Marasmius sphaerodermatoides Singer is morphologically similar to *C. ligustrumae* and also grow on the dead leaves of *Ligustrum* (Singer, 1989). However, the two species are distinguished that *M. sphaerodermatoides* has two dimorphous dermatocystidia on the stipe, the other is 23 × 8 µm, ampullaceous and one is 11 × 4.2 µm, clavate or cylindrical (Singer, 1989) that those of *C. ligustrumae* are absent.

Table 3: Morphlogical comparison of *C. ligustrumae* in this study and previous descriptions. "n/a" means information not available. Different characteristics to *C. ligustrumae* were shown in bold and underlined.

Compared species	Pileus		Number of lamellae	stipe		
	Size	Color		size	color	surface
C. ligustrumae	2-3 mm	dark brown to brown at centre light orange or light yellow towards margin sometimes yellowish-white or white at margin	7-10	10-30 × 0.15mm	brown, dark brown or black	spinose on the top
C. aucubae	1-7 mm	light brown, reddish brown or brownish orange at centre, light orange, orange white or whitish at margin	5-12	3-30 × 0.1-0.4 mm	reddish brown tp black	n/a
C. changchunensis	< 4 mm	**dark brown at centre, brown at margin**	**5-6**	10-40 × less than 1mm	**yellowish white to browinish orange to dark brown**	n/a
C. corbariensis	< 5 mm	darker, brick or cinnamon at centre and grooves paler, clay buff, buff or cream at margin	8-12	less than 30 × less than 0.5 mm	fuscous black to black usually paler purplish chestnut bay to milky coffee or clay burr in uppermost parts	n/a
C. crescentiae	4-10 mm	**beige-brown or daker**	**10-18**	5-20 × 0.2-0.4 mm	apex white, black elsewhere	setulose
C. minutus	0.6-2.5 mm	**pale red brown with a daker centre**	n/a	5-19.5 × 0.05-0.2 mm	brown to black brown	n/a
M. sphaerodermatoides	1.5-3.5 mm	**dark brown**	8-14	20 × 0.2 mm	chestnut	n/a

Table 3: continued.

Compared species	basidiospores			Size and shape of cystidia	
	size	Q values	shape	Cheilocystidia	Caulocystidia
C. ligustrumae	6.58-9.27 × 3.82-5.05 μm	1.81	elongate	a) 16-32 × 4-10 μm subfusiform, lageniform, subcylindrical, rostrate b) 10-25 × 7-15 μm Rotails-type broom cells, clavate, pyriform	2.44-16.17 × 1.29-4.91 μm subulate
C. aucubae	**7-10 × 2.5-4.2 μm**	**1.71-2.8**	ellipsoid to ellipsoid-fusoid	a) 16-32 × 4-10 μm subfusiform, lageniform, subcylindrical, rostrate b) 10-25 × 7-16 μm Rotails-type broom cells, clavate, pyriform	5.2-21 × 2-5 μm subcylindrical, lageniform
C. changchunensis	**5.9-7.6 × 2.3-3.6 μm**	**2.1-2.77**	ellipsoid -fusoid, oblong, subcylindrical	a) 18-32 × 4-9 μm subfusiform, narrowly utriform, lageniform, subcapitate subcylindrical b) 9-20 × 4-16 μm Rotails-type broom cells, clavate	10-20 × 3-7 μm subcylingrical, lageniform, subcapitate, subcylindrical
C. corbariensis	8.2-10.7 × 3.8-5.0 μm	1.8-2.5	ellipsoid to cylindrical	a) 21.5-32.5 × 3.5-6 μm fusiform b) 14-17.5 × 6-9.5 μm pedunculate pyriform	**not seen but small up to 3 μm long projections present occasionally**
C. crescentiae	**6.5 × 2.7 μm**	n/a	ellipsoid to amygdaliform	a) 25-35 × 4-10 μm fusoid to fusoid-mucronate b) 20-25 × 8-14 μm Rotails-type cells, clavate to utriform	**absent**
C. minutus	**6-8 × 2.2-4 μm**	n/a	ellipsoid to narrowly ellipsoid	a) 20-31 × 6.5-13 μm fusiform, lageniform b) 10-16.5 × 6-11 μm Rotails-type broom cells, clavate to vesiculose	**absent**
M. sphaerodermatoides	7-8 × 3.5-4.2 μm	n/a	ellipsoid	11-23 × 9-17.5 μm Rotails-type, obpyriform or globose	**a) 23 × 8 μm** **ampullaceous** **b) 11 × 4.2 μm** **clavate or cylindrical**

Table 3: continued.

Compared species	Pileipellis a hymeniderm		Basidiole		References
	size	shape	size	shape	
C. ligustrumae	11.9-23.6 × 8.4-14.4 µm	Rotails-type broom cells, napiform to turbinate	16.5-21.1 × 4.37-6.21 µm	subulate to clavate	
C. aucubae	7-34 × 4-27 µm	Rotails-type broom cells, subglobose, clavate, pyriform	15-24 × 4-8 µm	subfusiform, clavate	Neda and Doi (1998) Kiyashko et al. (2014) Li and Bau (2024)
C. changchunensis	10-27 × 5-18 µm	Rotails-type broom cells, subglobose, clavate	11-15 × 4-5 µm	subfusiform, clavate	Li and Bau (2024)
C. corbariensis	12.5-20 × 8.5-12.5 µm	peduculate spherical and pyriform	n/a	n/a	Bozok et al. (2018)
C. crescentiae	10-20 × 8-16 µm	Rotails-cells, clavate to glogose	n/a	n/a	Desjardin and Horak (1997) Kiyashko et al. (2014)
C. minutus	10-21 × 6-15 µm	Rotails-type broom cells, clavate to pyriform	11-19 × 3.5-8.5 µm	cylindrical-clavate to clavate	Kaplan et al. (2021)
M. sphaerodermatoides	11-23 × 9-17.5 µm	Rotails-type, obpyriform or globose	n/a	n/a	Singer (1989)

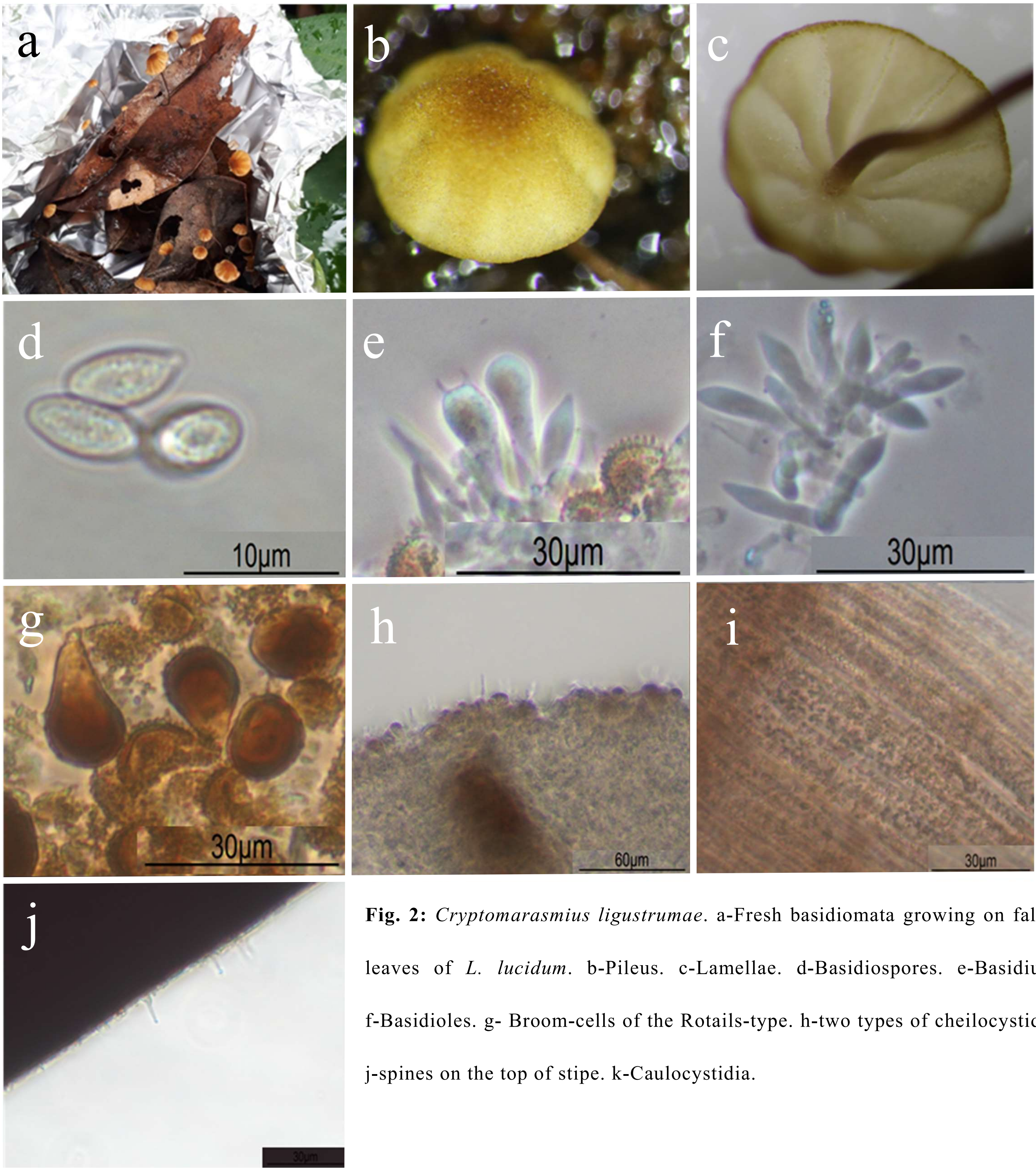

Fig. 2: *Cryptomarasmius ligustrumae*. a-Fresh basidiomata growing on fallen leaves of *L. lucidum*. b-Pileus. c-Lamellae. d-Basidiospores. e-Basidium. f-Basidioles. g- Broom-cells of the Rotails-type. h-two types of cheilocystidia. j-spines on the top of stipe. k-Caulocystidia.

Cryptomarasmius hederae **E. Ito, sp. nov. (ad interim)**

Fig. 3

Pileus 1 mm broad, hemispherical when young, convex-expanded, slightly depressed when mature, very shallowly sulcate (S = 4-6), sometimes a little distorted, surface dry, glabrous, initially dark brown to brown overall, turns light orange to light yellow or brown towards margin, brown or dark brown overall when dry, hygroscopic. Context very thin, cream. Lamellae under 1 mm wide, white or translucently white, remote or adnexed, distant (L = 4-6). Stipe under 10 mm long, 0.08 mm wide, central, cylindrical, wiry, often tortuous but pileus upward, equal, surface brown, dark brown or black overall, light orange or light yellow towards pileus, smooth, insititious. Rhizomorphs absent. Odor not distinctive.

Basidiospores (7.03–) 8.99 (–10.81) × (3.79–) 4.78 (–5.79) µm, Q = 1.89, elongate, slightly curved toward germ pore, thin-walled, smooth, hyaline. Basidioles 15.7-24.5 × 5.00-7.70 µm subulate to clavate, smooth, sometimes with papilla. Pileipellis a hymeniderm, broom-cells of the Rotails-type, 11.9-23.6 × 8.4-14.4 µm, napiform to turbinate, pale brown, brown to dark brown on the top, achroic, pale yellow of pale brown on the bottom, spinose (spines < 1 µm) on the top, smoot on the bottom, thick-walled. Caulocystidia 14.5-14.9 × 4.37-5.83 µm, lageniform, sometimes capitate, smooth, hyaline.

Habit and Habitat: Solitary or gregarious on fallen leaves and branches of *H. helix*, *H. rhombea* and *M. grandiflora*. Growing in garden or mixed forest during all seasons, mostly rainy season and summer.

Holotype: JAPAN, Tokyo, Minato, Mita, Mita Campus of Keio University, scattered on fallen leaves of *H. helix* in the garden, May 17, 2024, Eisaburo Ito (15).

Etymology: The epithet refers to the genus of the Japanese plant, *H. rhombea*, the host plant of the new species.

Additional specimens examined: Japan: Kanagawa, Yokohama, Kohoku, Hiyoshi, Hiyoshi Campus of Keio University, fallen leaves *H. rhombea* in the mixed forest dominated by *Q. serrata* and *L. lucidum*, July 2, 2024, Shohei Wada (42). Tokyo, Minato, Mita, Mita Campus of Keio University, fallen leaves of *M. grandiflora* in the garden, June 28, 2024, Eisaburo Ito (47).

Observations: *Cryptomarasmius hederae* is characterized by its very small pileus (less than 1 mm broad) colored dark brown to brown on the top and light orange to light yellow or brown towards margin, distant lamellae (L = 4-6), short stipe (< 10 mm), basidiospores measuring 8.99 × 4.78 µm (without germ pore), presence of caulocystidia. In addition, this is characterized by their host plants, growing on fallen leaves and stems of *H. helix*, *H. rhombea* and *M. grandiflora*.

Cryptomarasmius sp., the Japanese specimens (B5000, B5070 and B5442) collected from fallen leaves of *P. tobira* are phylogenetically close to *C. hederae*. However, these two species can be distinguished in that *Cryptomarasmius* sp. does not have caulocystidia (Kasuya et al. 2024).

Cryptomarasmius exustoides is also phylogenetically close to *C. hederae*. However, the two species can be distinguished in that *C. exustoides* has bigger pileus (1-4 mm) and does not have caulocystidia (Desjardin and Horak 1997, Dutta and Acharya 2018).

Aron (2020) described the specimens growing on fallen leaves of *H. helix* as *C. corbariensis*. However. *C. corbariensis* can be distinguished from *C. hederae* in that *C. corbariensis* has bigger pileus (up to 5 mm), developed lamellae (L = 8-12) and longer stipe (up to 30 mm) (Bozok et al., 2017).

Table 4: Morphological comparison of *C. hederae* in this study and previous descriptions. “n/a” means information not available. Different characteristics to *C. hederae* were shown in bold and underlined.

Compared species	Pileus		Number of lamellae	stipe	
	Size	Color		size	color
C. hederae	1 mm	dark brown to brown at centre light orange to light yellow or brown towards margin	4-6	10 × 0.08 mm	brown, dark brown or black
C. exustoides	**1-7 mm**	light brown, reddish brown or brownish orange at centre, light orange, orange white or whitish at margin	**5-12**	**3-30 × 0.1-0.4 mm**	reddish brown tp black
Cryptomarasmius sp.	< 2 mm	pale yellowish brown to yellowish brown	n/a	n/a	brown to dark brown
C. corbariensis	**< 5 mm**	darker, brick or cinnamon at centre and grooves paler, clay buff, buff or cream at margin	**8-12**	**less than 30 × less than 0.5 mm**	fuscous black to black usually paler purplish chestnut bay to milky coffee or clay burr in uppermost parts

Table 4: continued.

Compared species	basidiospores		
	size	Q values	shape
C. hederae	7.03-10.81 × 3.79-5.79 µm	1.89	elongate
C. exustoides	7-10 × 2.5-4.2 µm	1.71-2.8	ellipsoid to ellipsoid-fusoid
Cryptomarasmius sp.	7-10 × 4-5 µm	n/a	ellipsoid -fusoid, oblong, subcylindrical
C. corbariensis	8.2-10.7 × 3.8-5.0 µm	1.8-2.5	ellipsoid to cylindrical

Table 4: continued.

Compared species	Size and shape of cystidia	
	Cheilocystidia	Caulocystidia
C. hederae	not observed	14.5-14.9 × 4.37-5.83 µm lageniform
C. exustoides	a) 16-32 × 4-10 µm subfusiform, lageniform, subcylindrical, rostrate b) 10-25 × 7-16 µm Rotails-type broom cells, clavate, pyriform	**absent**
Cryptomarasmius sp.	a) 23-39 × 4-7 µm subfusiform, narrowly utriform, lageniform, subcapitate subcylindrical b) 14-27 × 6-11 µm Rotails-type broom cells, clavate	**absent**
C. corbariensis	a) 21.5-32.5 × 3.5-6 µm fusiform b) 14-17.5 × 6-9.5 µm pedunculate pyriform	**not seen but small up to 3 µm long projections present occasionally**

Table 4: continued.

Compared species	Pileipellis a hymeniderm		Basidiole		References
	size	shape	size	shape	
C. hederae	11.9-23.6 × 8.4-14.4 µm	Rotails-type broom cells, napiform to turbinate	15.7-24.5 × 5.00-7.70 µm	subulate to clavate	
C. exustoides	7-34 × 4-27 µm	Rotails-type broom cells, subglobose, clavate, pyriform	15-24 × 4-8 µm	subfusiform, clavate	Desjardin and Horak (1997) Dutta and Acharya (2018)
Cryptomarasmius sp.	15-225 × 7-12 µm	Rotails-type broom cells, subglobose, clavate	n/a	n/a	Kasuya et al. (2024)
C. corbariensis	12.5-20 × 8.5-12.5 µm	peduculate spherical and pyriform	n/a	n/a	Bozok et al. (2018)

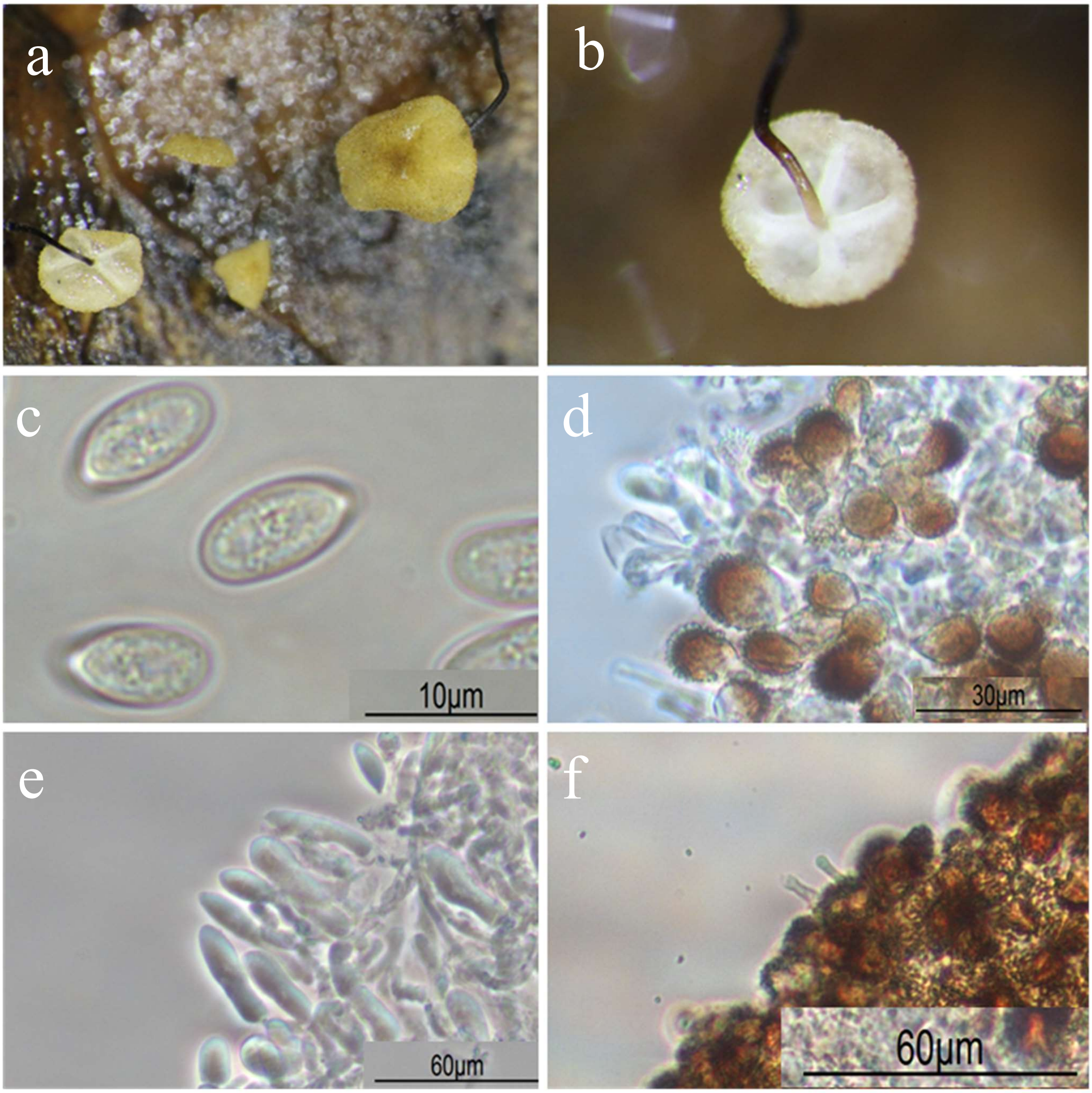

Fig. 3: *Cryptomarasmius hederae*. a-Flesh basidiomata. b-Lamellae. c-Basidiospores. d- Broom-cells of the Rotails-type. e-Basidioles. f-Cheilocystidia or pileocystidia

Cryptomarasmius hispidus **E. Ito, sp. nov. (ad interim)**

Fig. 4

Pileus 3-4 mm broad, hemispherical or subconical when young, convex-expanded, slightly depressed when mature, plicate (S = 14-17), surface dry, hirtose overall especially at top and margin gathering and becoming like spine, initially dark brown or black overall, turns brown or dark brown towards margin, white or light yellow at sulci, dark brown or black overall when dry, hygroscopic. Context thin, cream. Lamellae 1 mm wide, white overall, brown at margin, distant (L = 14-17). Stipe 20-40 mm long, 1 mm thick, central, cylindrical, wiry, sometimes a little tortuous but pileus upward, equal, surface black overall, smooth, insititious. Rhizomorphs absent. Odor not distinctive.

Basidiospores (6.97–) 8.06 (–9.18) × (4.36–) 4.97 (–5.81) μm, Q = 1.62, ellipsoid-elongate, slightly curved toward germ pore, thin-walled, smooth, hyaline, amyloid. Basidioles 15.44-23.13 × 4.21-8.39 μm, subulate to clavate, smooth, sometimes with papilla. Pileipellis a hymeniderm of two types: a) broom-cells of the Rotails-type 16.8-24.8 × 9.03-15.5 μm, napiform to turbinate, pale brown, brown or dark brown at the top, achroic, pale yellow or pale brown at the bottom, spinose (spines < 1 μm) on the top, smooth at the bottom, thick-walled, sometimes vertically concrescent; b) chains 70.5-116.1 × 6.33-10.1 μm, fusoid to cylindric, subulate at the tip, pale brown to brown, few spinose (spines < 1 μm), thick-walled. Hair on pileus (3.47–) 5.10 (–9.41) μm broad, dendrohyphidium with spines (< 2 μm) and projections like pileipellis cells of type a (6.51-18.5 × 6.10-15.3 μm), nodulose, brown, thin-walled. Cheilocystidia of two types: a) 11.52-19.31 × 6.35-10.0 μm, napiform to turbinate, pale brown at the top, achoroic at the bottom, spinose (spines < 1 μm) on the top, smooth at the bottom, thick-walled; b) 17.35-26.98 × 5.07-7.16 μm, lageniform to tibiiform, smooth. Caulocystidia absent; stipe surface covered by a brown amorphous layer.

Habit and Habitat: Solitary or sparse on fallen leaves and branches of *M. grandiflora* and fallen branches of *H. helix*. Growing in garden during spring, rainy season.

Holotype: JAPAN, Tokyo, Minato, Mita, Mita Campus of Keio University, scattered or solitary on fallen leaves and branches of *M. grandiflora* in the garden, April 24, 2024, Eisaburo Ito (B5213).

Etymology: The epithet refers to the characteristic hair on the pileus of the new species.

Additional specimen examined: Japan: Tokyo, Minato, Mita, Mita Campus of Keio University, fallen branches of *H. helix* in the garden, April 24, 2024, Eisaburo Ito (B5218).

Observations: *Cryptomarasmius hispidus* is characterized by pileus colored dark brown or black at the top and brown or dark brown towards margin with hair especially on the top and at the margin gathering and becoming like spine, distant and developed lamellae (L = 14-17), thicker basidiospores (8.06 × 4.97 μm) pileipellis a hymeniderm of chain type, two types of cheilocystidia, stipe covered by a brown amorphous layer. In addition, this is characterized by their host plants, growing on fallen leaves and stems of *M. grandiflora* and fallen stems of *H. helix*.

Cryptomarasmius thwaitesii is phylogenetically close to *C. hispidus*. However, the sizes of the basidiospores of *C. thwaitesii* were 6.5-10 × 3.3-4.5 (–5.5) μm and Q value was 1.9 (Antonin, 2007). In Puccinelli and Capelari (2009), the size was 6.2-10 × 3.7-4.2 μm and Q value was 2.2. In addition, the color of pileus of *C. thwaitesii* is same to its stipe (Antonin, 2007). In other words, the two species distinguished in that the basidiospores of *C. hispidus* are thicker than that of *C. thwaitesii* and the color of stipe of *C. hispidus* is much darker than of its pileus. In phylogenetic analysis, the Japanese specimens (B5213 and B5218) were placed within a clade with *C. thwaitesii* collected from China (HMJAU 68267 and HMJAU 68268). The sequence data of these Chinese specimens was newly deposited to GenBank in 2024 by Li and Bau (2024). In Li and Bau (2024), these two specimens formed a sister clade with the specimens of *C. thwaitesii* (DED 5918 added Jenkinson et al., 2014 and LF 2131 added in 2018) but they were not described these morphological features. In the present study, the differences of the sizes of basidiospores and the colors of pileus and stipe suggest that the two Japanese specimens are different from *C. thwaitesii*. This results also suggest that the Chinese specimens (HMJAU 69267 and HMJAU 68268) are not identical with *C. thwaitesii* and same to the present new species.

Cryptomarasmius magnoliae (Singer) T.S. Jenkinson & Desjardin is morphologically similar to *C. hispidus* and also grows on fallen leaves and branches of *M. grandiflora*. However, the two species can be distinguished in that the sizes of the basidiospores of *C. magnoliae* is narrower (8.7-9.3 × 3.5-4.3 μm, most frequently 8.8-9 × 4.4.2 μm) (Singer, 1976). Moreover, *C. magnoliae* differs from *C. hispidus* in the pileus with fimbriate-ciliate only at margin (not at the top).

Cryptomarasmius kroumirensis (Pat.) T.S. Jenkinson & Desjardin is also morphologically similar to *C. hispidus*. However, the two species can be distinguished in that *C. kroumirensis* has thicker basidiospores (6-9 × 3-3.5 μm) and have spines only at the top (not at the margin) (Singer, 1976).

However, there are no sequence data of *C. magnoliae* and *C. kroumirensis* in the database so the additional studies on their phylogenetic placements are required.

Table 5: Morphological comparison of *C. hispidus* in this study and previous descriptions. “n/a” means information not available. Different characteristics to *C. hispidus* were shown in bold and underlined.

Compared species	Pileus			Number of lamellae
	Size	Color	Surface	
C. hispidus	3-4 mm	dark brown or black at centre brown to dark brown towards margin	hitose overall, especially at the top and margin	14-17
C. kroumirensis	**1mm**	brown brown echinulate in apical portion	**echinulate at the top**	8-11
C. magnoliae	< 5.5 mm	deep brown	**pale buff at the margin**	n/a
C. thwaitesii	1.5-5 mm	dark reddish chestnut brown	echinulate-spinulose fimbriate at the margin	10-17

Table 5: continued.

Compared species	stipe			basidiospores		
	size	color	surface	size	Q values	shape
C. hispidus	20-40 × 1 mm	black	covered by a brown amorphous layer	6.97-9.18 × 4.36-5.81 µm	1.62	ellipsoid to elongate
C. kroumirensis	5-18 × 0.1-0.2 mm	black	many telepods present	**6-9 × 3-3.5 µm**	n/a	n/a
C. magnoliae	10-40 × 0.2-0.5 µm	blackish brown	n/a	**8.7-9.3 × 3.5-4.3 µm**	n/a	ellipsoid-fusoid
C. thwaitesii	3-30 × 0.2-1 mm	**chestnut brown concolorous with pileus**	stipe surface covered by a brown amorphous layer	**6.5-10 × 3.3-5.5 µm**	**1.9-2.2**	ellipsoid , subfusoid to amugdaliform, olong-fusiform

Table 5: continued.

Compared species	Size and shape of cystidia		Pileipellis a hymeniderm	
	Cheilocystidia	Caulocystidia	size	shape
C. hispidus	a) 17.35-26.98 × 5.07-7.16 µm lageniform to tibiiform b) 11.52-19.31 × 6.35-10.01 µm Rotails-type broom cells, napiform to turbinate	absent	a) 16.8-24.8 × 9.03-15.5 µm b) 70.5-116.1 × 6.33-10.1 µm	a) Rotails-type broom cells, napiform to turbinate b) fusoid to cylindric, subulate at the top
C. kroumirensis	like pileipellis a hymeniderm	n/a	8-15 × 4.5-10 µm	Rotails-type broom cells, hymeniform
C. magnoliae	4-7 µm fusoid	n/a	11-40 × 7-17 µm	claviate
C. thwaitesii	a) 24-44 × 3.7-8.5 µm lageniform to fusoid, ampullaceous b) 17.5-26 × 5.2-11.5 µm Rotails-type broom cells, clavate, cylindrical	absent	a) 15-36 × 9.0-19 µm b) 11.5-50 × 5.5-12 µm	a) Rotails-type broom cells, clavate b) fusoid, limoniform, ellipsoid

Table 5: continued.

Compared species	Basidiole		References
	size	shape	
C. hispidus	15.44-23.13 × 4.21-8.39	subulate to clavate	
C. kroumirensis	n/a	short-fusoid-mucronate	Singer (1976)
C. magnoliae	n/a	n/a	Singer (1976)
C. thwaitesii	15-31 × 3.5-8.0 µm	clavate to subcylindrical	Antonin (2007) Puccinelli and Capelari (2009)

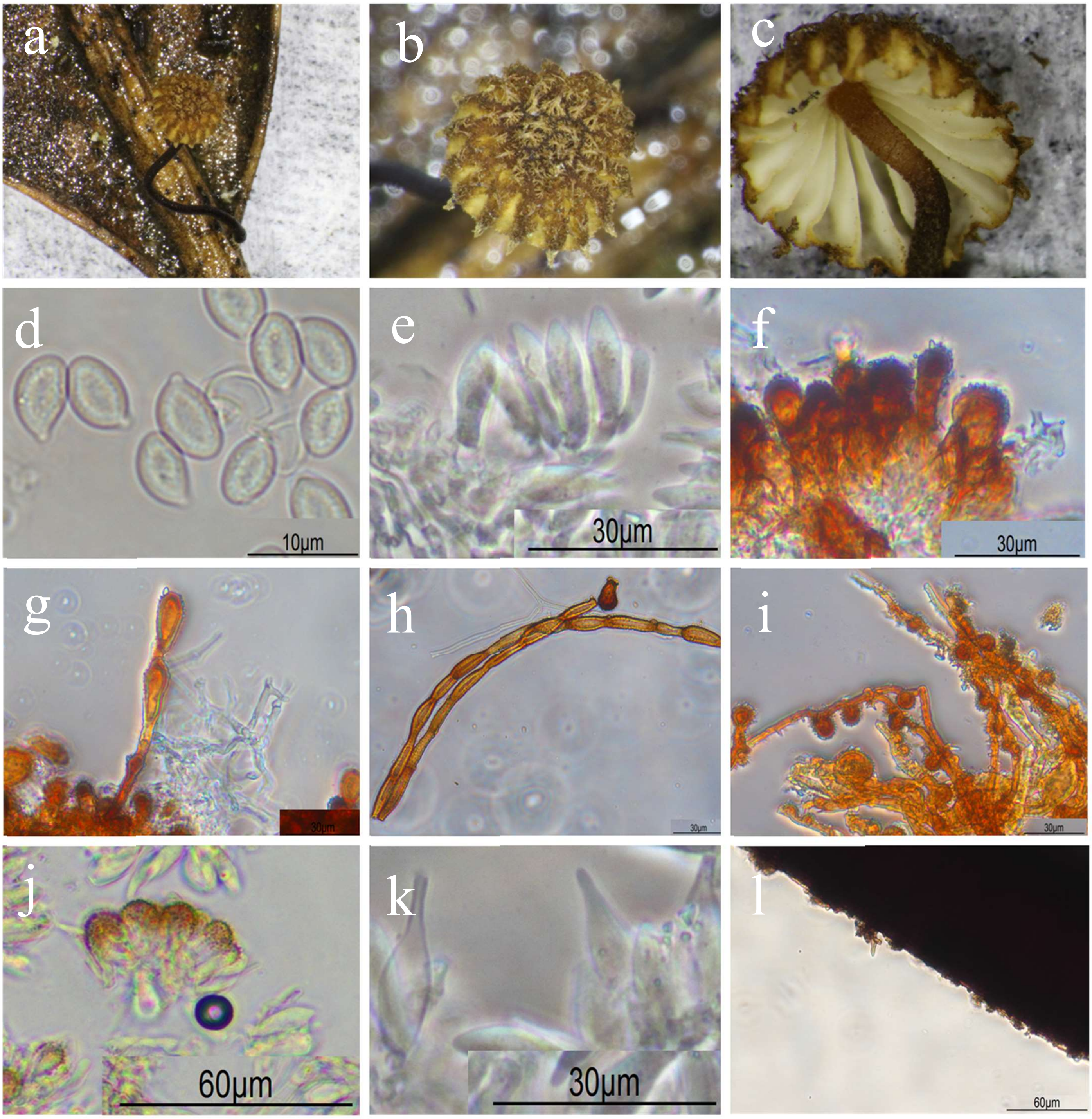

Fig. 4: *Cryptomarasmius hispidus*. a-Fresh basidiomata b-Pileus. c-Lamellae. d-Basidiospores. e-Basidioles. f-broom-cells of the Rotails-type. g-Combining broom-cells. h-Chains. i-Hairs at the pileus. j-Cheilocystidia type a. k-Cheilocystidia type b. l- Brown amorphous layers.

Cryptomarasmius exustoides **(Desjardin & E. Horak) T.S. Jenkinson & Desjardin, Mycologia 106(1): 92 (2014)**

Fig. 5

Pileus 3-4 mm broad, hemispherical or conical when young, convex-expanded, slightly depressed when mature, sulcate or shallowly sulcate (S = 9-10), sometimes a little distorted, surface dry, glabrous, initially dark brown or brown overall, turns white, pale yellow or brown towards margin, white or pale yellow at sulci, brown or dark brown overall when dry, hygroscopic. Context very thin, cream. Lamellae 1 mm wide, white, remote or adnexed, distant (L = 6-10). Stipe 10-30 mm long, 0.12 mm broad, central, cylindrical, wiry, often tortuous but pileus upward, equal, surface dark brown or black, overall, smooth, insititious. Rhizomorphs absent. Odor not distinctive.

Basidiospores (7.80–) 8.88 (–10.59) × (4.48–) 5.12 (–5.80) µm, Q = 1.74, elongate, slightly curved toward germ pore, thin walled, smooth, hyaline, amyloid. Basidioles 19.8-26.1 × 7.06-9.42 µm, subulate to clavate, smooth, sometimes with papilla. Pileipellis a hymeniderm, broom-cells of the Rotails-type, 11.60-24.17 × 7.40-12.52 µm, turbinate to clavate, pale brown, brown to dark brown on the top, achroic, pale yellow of pale brown on the bottom, spinose (spines < 2 µm) on the top, smoot on the bottom, thick-walled. Caulocystidia rarely present, 11.6-13.6 × 1.40-2.26 µm, lageniform, sometimes capitate, smooth, hyaline.

Habit and Habitat: Solitary or gregarious on fallen aggregate follicles of *M. grandiflora*. Occur in garden during all seasons, mostly rainy season and summer.

Specimens examined: Japan: Tokyo, Minato, Mita, Mita Campus of Keio University, fallen aggregate follicles of *M. grandiflora* in the garden, April 26, 2024, Eisaburo Ito (B5214 and B5219). Same place, fallen aggregate follicles of *M.*

grandiflora in the garden, June 28, 2024 Eisaburo Ito (49).

Observations: *Cryptomarasmius exustoides* is characterized by tiny and small pileus colored brown or dark brown on the top and white, pale yellow or brown at margin, distant (L = 7-10) and white lamellae, tortuous, dark brown or black stipe, basidiospores measuring 8.88 × 5.12 µm (without germ pore), rarely present or absence of caulocystidia. In addition, this species is characterized by their host plants, growing on fallen aggregate follicles of *M. grandiflora* in Japan.

Aforementioned morphological features match with the description of *C. exustoides* (Desjardin and Horak, 1997; Dutta and Acharya, 2018; the sizes of basidiospores of Japanese specimens are smaller than previous descriptions because Japanese specimens were measured without germ pore). The Japanese specimens have the wide variation of pileus color and these color match the above previous descriptions. Previously, *C. exustoides* were collected from New Zealand (Desjardin and Horak, 1997), Hawaii (Jenkinson et al., 2014) and India (Dutta and Acharya, 2018) and the known host plant is the plant of *Cordyline* spp. (Agavaceae) (Desjardin and Horak, 1997). This is the first record of *C. exustoides* in Japan and, the first record of *M. grandiflora* as its host plant.

Cryptomarasmius sp. collected on *P. tobira* in Japan (B5000, B5070 and B5442) are phylogenetically close to *C. exustoides*. However, the two species can be distinguished in that Cryptomarasmius sp. has smaller pileus (up to 2 mm).

Cryptomarasmius micraster is also phylogenetically close to *C. exustoides*. However, the two species can be distinguished in that *C. micraster* has smaller pileus (1-2 mm), shorter stipe (10-18 mm) and longer basidioles (32-40 × 8-10 µm) (Tan et al., 2009).

Cryptomarasmius hederae is phylogenetically close to *C. exustoides* but they are morphologically different as mentioned above.

Table 6: Morphological comparison of *C. exustoides* in this study and previous descriptions. "n/a" means information not available. Different characteristics to *C. exustoides* were shown in bold and underlined.

Compared species	Pileus		Number of lamellae	stipe	
	Size	Color		size	color
C. exustoides (japanese specimens)	3-4 mm	dark brown or brown at centre white, pale yellow or brown towards margin	9-10	10-30 × 0.12 mm	dark brown to black
C. hederae	**1 mm**	dark brown to brown at centre light orange to light yellow or brown towards margin	**4-6**	**10 × 0.08 mm**	brown, dark brown or black
C. exustoides (foregin specimens)	1-7 mm	light brown, reddish brown or brownish orange at centre, light orange, orange white or whitish at margin	5-12	3-30 × 0.1-0.4 mm	reddish brown tp black
Cryptomarasmius sp.	**< 2 mm**	pale yellowish brown to yellowish brown	n/a	n/a	brown to dark brown
C. micraster	**1-2 mm**	pale grayish brown overall white at margin	n/a	**10-18 × 0.1 mm**	dark brown to black

Table 6: continued.

Compared species	basidiospores			Size and shape of cystidia	
	size	Q values	shape	Cheilocystidia	Caulocystidia
C. exustoides (japanese specimens)	7.80-10.59 × 4.48-5.80 µm	1.74	elongate	not observed	11.6-13.6 × 1.40-2.26 µm rarely present, lageniform
C. hederae	7.03-10.81 × 3.79-5.79 µm	1.89	elongate	a) 16-32 × 4-10 µm subfusiform, lageniform, subcylindrical, rostrate b) 10-25 × 7-15 µm Rotails-type broom cells, clavate, pyriform	**14.5-14.9 × 4.37-5.83 µm lageniform**
C. exustoides (foregin specimens)	7-10 × 2.5-4.2 µm	1.71-2.8	ellipsoid to ellipsoid-fusoid	a) 16-32 × 4-10 µm subfusiform, lageniform, subcylindrical, rostrate b) 10-25 × 7-16 µm Rotails-type broom cells, clavate, pyriform	absent
Cryptomarasmius sp.	7-10 × 4-5 µm	n/a	ellipsoid -fusoid, oblong, subcylindrical	a) 23-39 × 4-7 µm subfusiform, narrowly utriform, lageniform, subcapitate subcylindrical b) 14-27 × 6-11 µm Rotails-type broom cells, clavate	absent
C. micraster	9-13 × 4.5-7 µm	1.6-2.8	ellipsoid	a) 30-36 × 7-12 µm clavate to cylindrical, fusoid b) 33-60 × 7-12 µm Rotails-type broom cells, subclavate, to clavate or subglobose	absent

Table 6: continued.

Compared species	Pileipellis a hymeniderm		Basidiole		References
	size	shape	size	shape	
C. exustoides (japanese specimens)	11.60-24.17 × 7.40-12.52 μm	Rotails-type broom cells, turbinate to clavate	19.8-26.1 μm	subulate to clavate	
C. hederae	11.9-23.6 × 8.4-14.4 μm	Rotails-type broom cells, napiform to turbinate	15.7-24.5 × 5.00-7.70	subulate to clavate	
C. exustoides (foregin specimens)	7-34 × 4-27 μm	Rotails-type broom cells, subglobose, clavate, pyriform	15-24 × 4-8 μm	subfusiform, clavate	Desjardin and Horak (1997) Dutta and Acharya (2018)
Cryptomarasmius sp.	15-225 × 7-12 μm	Rotails-type broom cells, subglobose, clavate	n/a	n/a	Kasuya et al. (2024)
C. micraster	17-30 × 8-22 μm	Rotails-type broom cells, clavate to subglobose	**32-40 × 8-10 μm**	clavate	Tan et al. (2009)

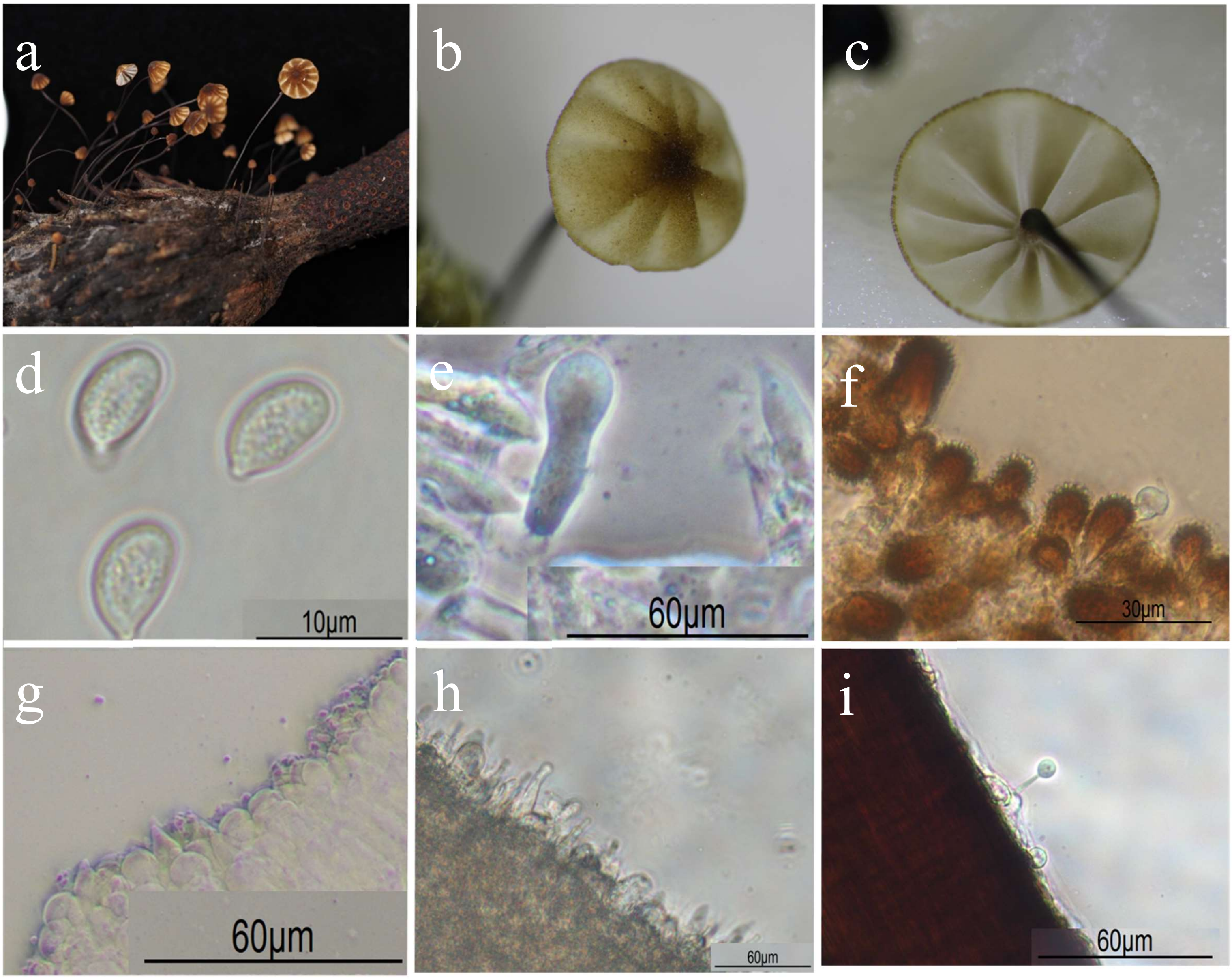

Fig. 5: *Cryptomarasmius exustoides*. a-Flesh basidiomata. b-Pileus. c-Lamellae. d-Basidiospores. e-Basidioles. f-Broom-cells of the Rotails-type. g-pleurocystidia. h-Two types of cheilocystidia. i-Caulocystidia

2.4. Conclusions of taxonomic study

This study revealed that there are two species of *Cryptomarasmius* growing on the dead leaves of *O. europaea* in the world. This result shows that *Cryptomarasmius* cannot be identified only by their host plant species. This is supported by recent descriptions of *C. aucubae*. *Cryptomarasmius aucubae* is firstly reported by Neda and Doi (1998) as a species that specific grows on the fallen leaves and twigs of *A. japonica*. However, according to Kiyashko et al. (2014), *C. aucubae* also grows on the fallen leaves of *Phellodendron amurense*. According to Li and Bau (2024), *C. aucubae* also grows on the fallen leaves of *Q. mongolica* and *Ulmus pumila*. *Phellodendron amurense* also grows in Japan but there are no reports in the country as the host plants of *C. aucubae*. This suggests that the host plants of the species of *Cryptomarasmius* possibly variable by geographic distribution.

Cryptomarasmius ligustrumae grows on the fallen leaves of *L. japonicum, L. lucidum* and *O. europaea* all of which belong to the tribe of *Oleae* in the family *Oleaceae*. Therefore, these plants are taxonomically close. In contrast, *C. aucubae* and *C. hederae* grow on multiple host plants which are taxonomically distant from each other. This suggests that further studies on the relationships between *Cryptomarasmius* species, plants and geographical distributions are needed.

Ligustrum lucidum which is the host plant of *C. ligustrumae* is known as a global invasive species. According to Fernandez et al. (2020), *L. ligustrumae* widely spread by “a widespread human use mostly in urban and periurban settings, very abundant fruit and seed production, small bird-dispersed fruits, high germination rates, resprouting capacity, fast growth rates, low herbivory levels and tolerance to a wide range of light, temperature and soil”. This suspects that *C. ligustrumae* also spreads around the world with their host plant species. If *C. corbariensis* and *C. ligustrumae* are mixed in the same locality, these two species probably cannot be identified by its host and where they grow. Besides, there is a possibility either *C. corbariensis* or *C. ligustrumae* are probably driven out by losing interspecies competition. Physiological and ecological examinations about the relationships between these two species are needed.

The Japanese specimens of *C. exustoides* (49, B5214 and B5219) grew only on fallen aggregate follicles of *M. grandiflora*. At the locality of the specimens, there are also fallen leaves and branches of *M. grandiflora* and other specimens of *Cryptomarasmius* growing on them were collected (*C. hederae* and *C. hispidus*). Nevertheless, basidiomata of the Japanese specimens of *C. exustoides* are not observed on them. Some species of *Cryptomarasmius* are known to have host specificity but there were no reports of the species of *Cryptomarasmius* that grow only on plant bodies except leaves, barks and branches. This strong specificity of substrate suggests that the Japanese specimens of *C. exustoides* is probably the key species to reveal the mechanism of the host specificity of *Cryptomarasmius*. However, the specimens of *Cryptomarasmius* growing on *M. grandiflora* (47, 49, B5213, B5214 and B5219) were collected only at Mita Campus of Keio University. *Magnolia grandiflora* is native of North America, and is not native and only planted in Japan (Murata, 2014). Moreover, the areas where *M. grandiflora* is planted in Japan are mainly in parks and roadsides. These environment are often dry and there are few litters because the fallen leaves and branches are often artificially removed. The locality where the specimens collected also have few litters but is humid because of the thick growth of *H. helix* covered with the ground. In contrast, *C. hispidus* could culture from the spores of the specimen (B5213) collected after eight months. This specimen were collected at April 24, 2024 and stored in dry condition for eight months but these spores still alive. This suspects that the spores and basidiomata of *Cryptomarasmius* are strong to dried condition. Since many specimens collected in this study grew on non-native plants and obtained from the artificial habitats such as garden and planters, additional researches about the geographical origin of these fungi and their host plants, and the native habitats of these fungal species should be conducted.

In this study, three new species of *Cryptomarasmius* are described and one newly recorded species in Japan is reported. These species are recognized by morphological, ecological and phylogenetic characteristics. In the future, the author will try to obtain sequence data of other species of *Cryptomarasmius* described only by morphological characteristics and contribute to the progress of taxonomy of *Cryptomarasmius*.

3. Inoculation experiments

3.1. Materials and methods

The methods of culture experiment is the same as aforementioned (refer to 2. Classification research, 2.1. Material and method, 2.1.1. Specimens preparing and culture strains obtaining).

Specimens were collected from June 2024 to October 2024 from three sites in Japan indicated below (Table 7). These specimens were cultured and stored and DNA sequence data of the specimens were obtained and used for phylogenetic analyses as above way to identify the specimens.

In the field, healthy leaves were collected from the plants considered hosts of *Cryptomarasmius* spp. The six species of plants were collected from two sites in Japan indicated below (Table 8). Plants were selected that had no occurrence of basidiomata of *Cryptomarasmius* spp.

Leaves were divided into those with and without surface sterilization by ethanol (99.5%). In addition, these leaves were divided into those injured by dissecting needle and intact. Therefore, a total of 4 types of leaves were prepared (those with surface sterilization and injured, those with surface sterilization and intact, those without surface sterilization and injured, those without surface sterilization and intact). Cultured hyphae were put on these leaves. Types of inoculated hyphae and leaves were as below. In addition, leaves without inoculation of hyphae and surface sterilization were prepared and divided into those injured and intact for control. All leaves were onto water agar mediums in sterile Petri dishes and these petri dishes containing leaves were covered with lids and place indoor at 25 °C near windows.

Table 7: Inoculated species and targeted plants.

Culture No. (= Specimen No.)	Species	Locality	Leaves	Inoculated date
54 (= B5419)	*C. aucubae*	Kanagawa, Fujisawa, Kameino, Experiment Forest of Nihon University	*Aucuba japonica*	November 9, 2024
41 (= 42) / 45 (= 47)	*C. hederae*	Kanagawa, Yokohama, Kohoku, Hiyoshi, Hiyoshi Campus of Keio University	*Hedera rhombea*	August 26, 2024 / October 4, 2024
22 (= 24)	*C. ligustrumae*	Tokyo, Minato, Mita, Mita Campus of Keio University	*Aucuba japonica*	August 26, 2024
32 (= B5265)	*C. ligustrumae*	Tokyo, Minato, Mita, Mita Campus of Keio University	*Ligustrum lucidum*	October 4, 2024
36 (= B5212) / 32 (= B5265)	*C. ligustrumae*	Tokyo, Minato, Mita, Mita Campus of Keio University	*Olea europaea*	August 26, 2024 / October 2, 2024

Table 8: The plants from which healthy leaves were collected.

Plant	Locality	Collected date
Aucuba japonica	Kanagawa, Yokohama, Kohoku, Hiyoshi, Hiyoshi Campus of Keio University	August 26, 2024 November 9, 2024
Hedera rhombea	Kanagawa, Yokohama, Kohoku, Hiyoshi, Hiyoshi Campus of Keio University	August 26, 2024 October 4, 2024
Ligustrum lucidum	Tokyo, Minato, Mita, Mita Campus of Keio University	October 4, 2024
Olea europaea	Kanagawa, Yokohama, Kohoku, Hiyoshi, Hiyoshi Campus of Keio University	August 26, 30, 2024 October 2, 2024

3.2. Results

- ***Cryptomarasmius aucubae* to *Aucuba japonica***

For the injured leaves, the growth of hyphae in the injured area was visible to the naked eye (Fig. 6; also see following). Hyphae did not grow to outside of the injured area. The injured area of leaves died and the dead area spread gradually. In the dead area, leaves turned black. The spread of the dead part was not circular but spread widely along the main veins of the leaves, especially to the petiole. In the intact samples, there were not different reactions from the reaction of controls.

- ***Cryptomarasmius ligustrumae* to *Aucuba japonica***

For all leaves, the growth of hyphae was not visible to the naked eye (Fig. 7; also see following). There were not different reactions from the controls.

- ***Cryptomarasmius hederae* to *Hedera rhombea***

For the injured leaves, the growth of hyphae in the injured area was not visible to the naked eye but observed under a stereomicroscope (Fig. 8; also see following). The injured area of leaves died but the dead part did not spread widely (< 2 mm). In the dead area, some leaves turned black and some leaves turns light yellow or white. The dead area of leaves with surface sterilization spread a little wider than those without surface sterilization. In six of twenty injured leaves, the formation of the basidiomata suspected to *Cryptomarasmius* were observed. For only one intact leaf, the formation of the basidiomata suspected to *Cryptomarasmius* was observed. The basidiomata of the intact leaf occurred only from the peace of PDA medium but the basidiomata of the injured leaves formed from some points in the injured area. In the three intact leaves, there were not different reactions from the reaction of controls.

- ***Cryptomarasmius ligustrumae*** **to** ***Ligustrum lucidum***

For the injured leaves, the growth of hyphae in the injured area was visible to the naked eye (Fig. 9; also see following). Hyphae did not spread to outside of the injured area. The injured area of leaves died and the dead area spread gradually. In the dead area, leaves turned black or brown. The spread of the dead part was not circular but spread widely along the main veins of the leaves, especially to the petiole. In all injured leaves, the occurrences of the growth suspected to *Cryptomarasmius* were observed. The basidiomata grew not only from the points of the injured area but also from the points of the other area of these leaves. In the intact leaves, there were not different reactions from the reaction of controls.

- ***Cryptomarasmius ligustrumae*** **to** ***Olea europaea***

All leaves with surface sterilization died gradually from the edges of these leaves (Fig. 10; also see following). Therefore, the leaves with surface sterilization and without inoculation of hyphae were added and these leaves also died as same way. For the injured leaves without surface sterilization, the spread of hyphae in the injured area was visible to the naked eye. Hyphae spread to outside of the injured area and spread to outside of the leaves. The injured area of leaves died and the dead area spread gradually. This is different from the samples of *C. aucubae* to *A. japonica* and *C. ligustrumae* to *L. japonicum* in that the dead area of these samples spread along main veins of leaves. In the dead area, leaves turned black and brown. In two of four injured leaves without surface sterilization, the formations of the basidiomata suspected to *Cryptomarasmius* were observed. The basidiomata did not grow on the leaves but at the edge of the petri dish from hyphae. In the intact leaves without surface sterilization, there were not different reactions from the reaction controls.

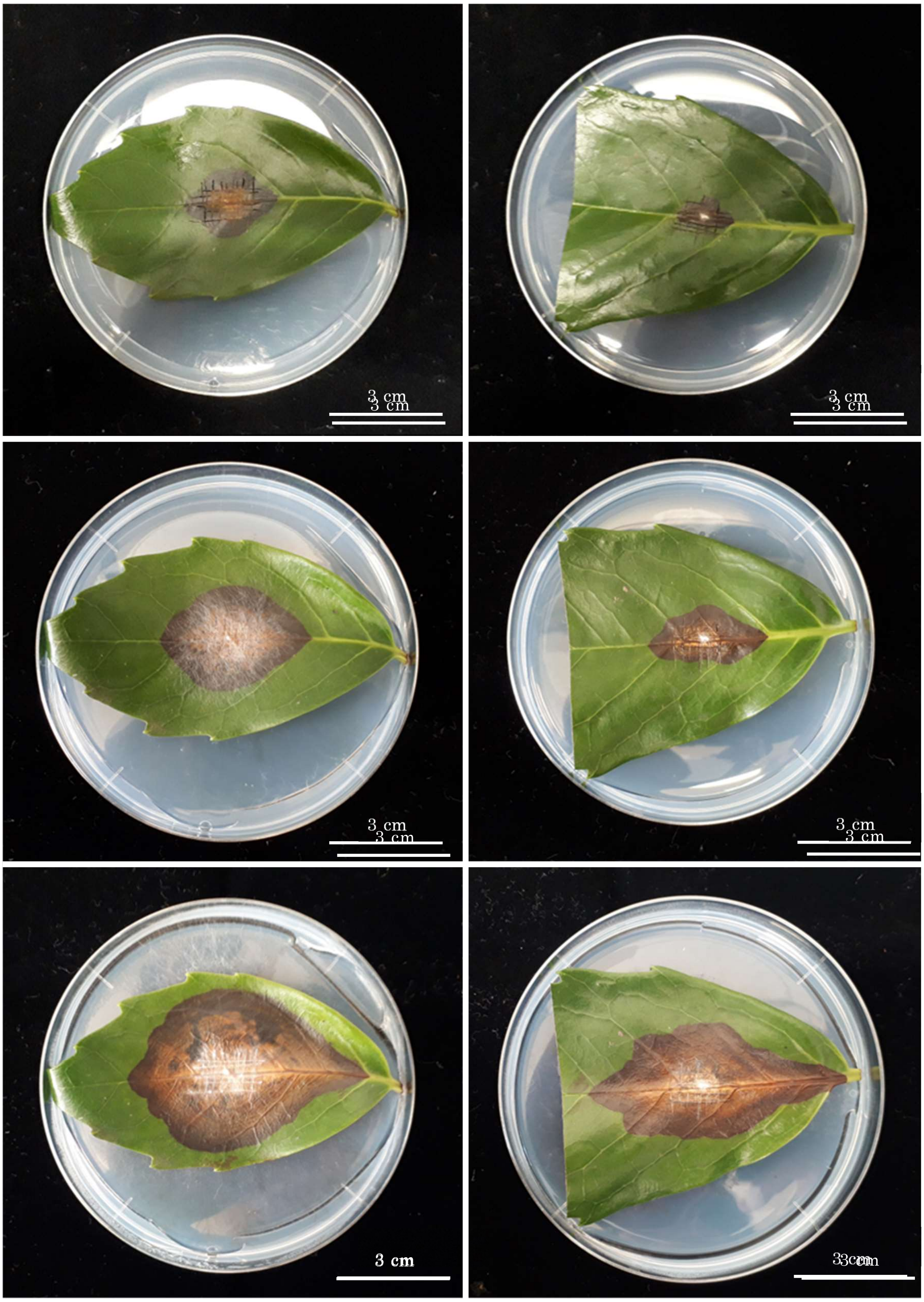

Fig. 6: *Cryptomarasmius aucubae* to *A. japonica*. Right leaves are injured with surface sterilization. Left leaves are injured without surface sterilization. Each leaf is after 8 days, 13 days, 22 days from the top.

Fig. 7: *Cryptomatasmius ligustrumae* to *A. japonica*. The two top leaves are injured with surface sterilization. The two middle leaves are injured and injured without surface sterilization. the bottom one is control. All leaves are after 49 days.

Fig. 8: *Cryptomarasmius hederae* to *H. rhombae*. The top one is injured with surface sterilization (after 17 days). The two below are injured without surface sterilization (middle one is after 25 days, bottom one is after 11 days). the photos right to leaves are enlarged surface and basidiomata.

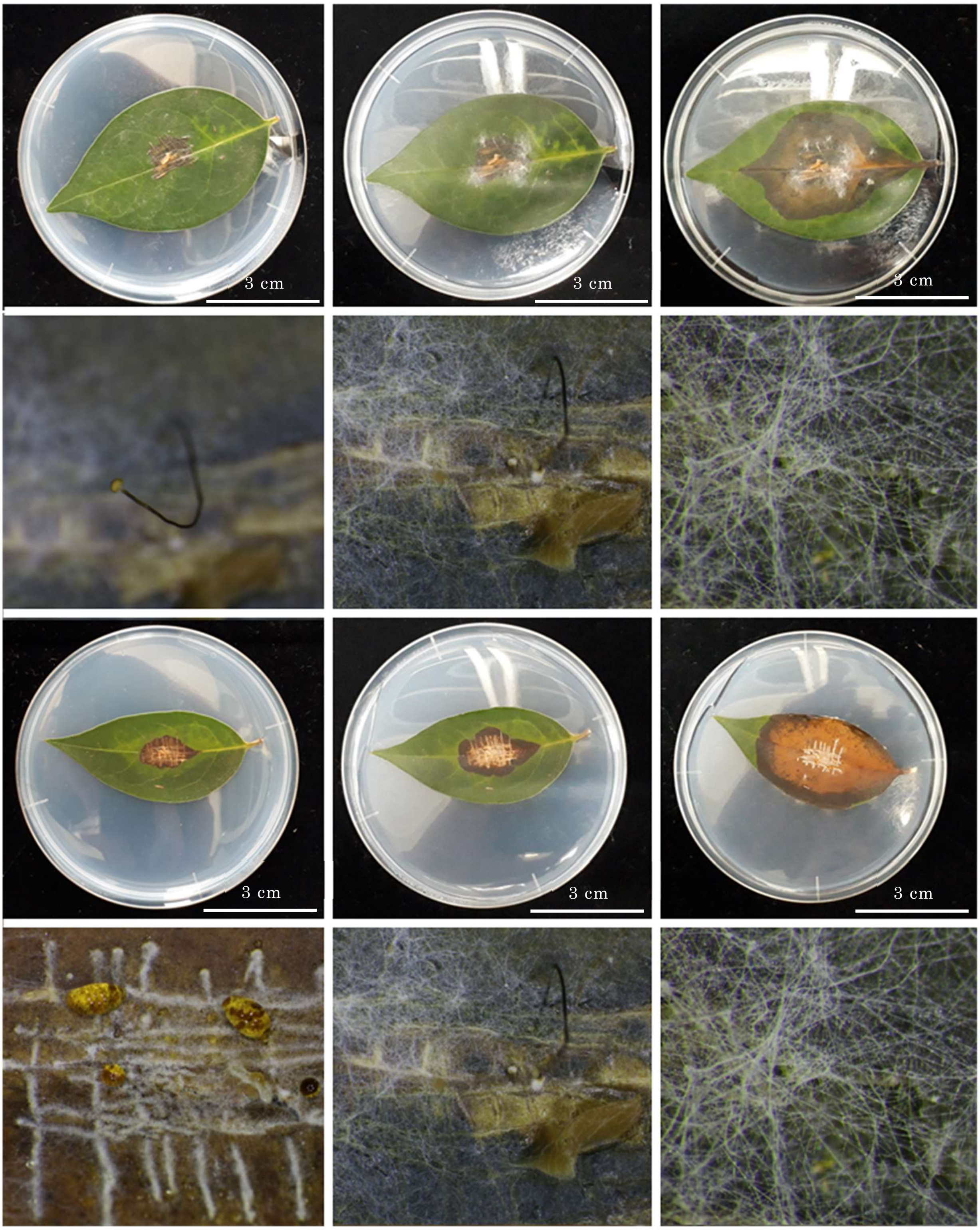

Fig. 9: *Cryptomarasmius ligustrumae* to *L. lucidum*. The above leaves are injured with surface sterilization. The below leaves are injured without surface sterilization. Photos under leaves are enlarged surface and basidiomata. Each leaf is after 10 days, 13 days, 25 days from left.

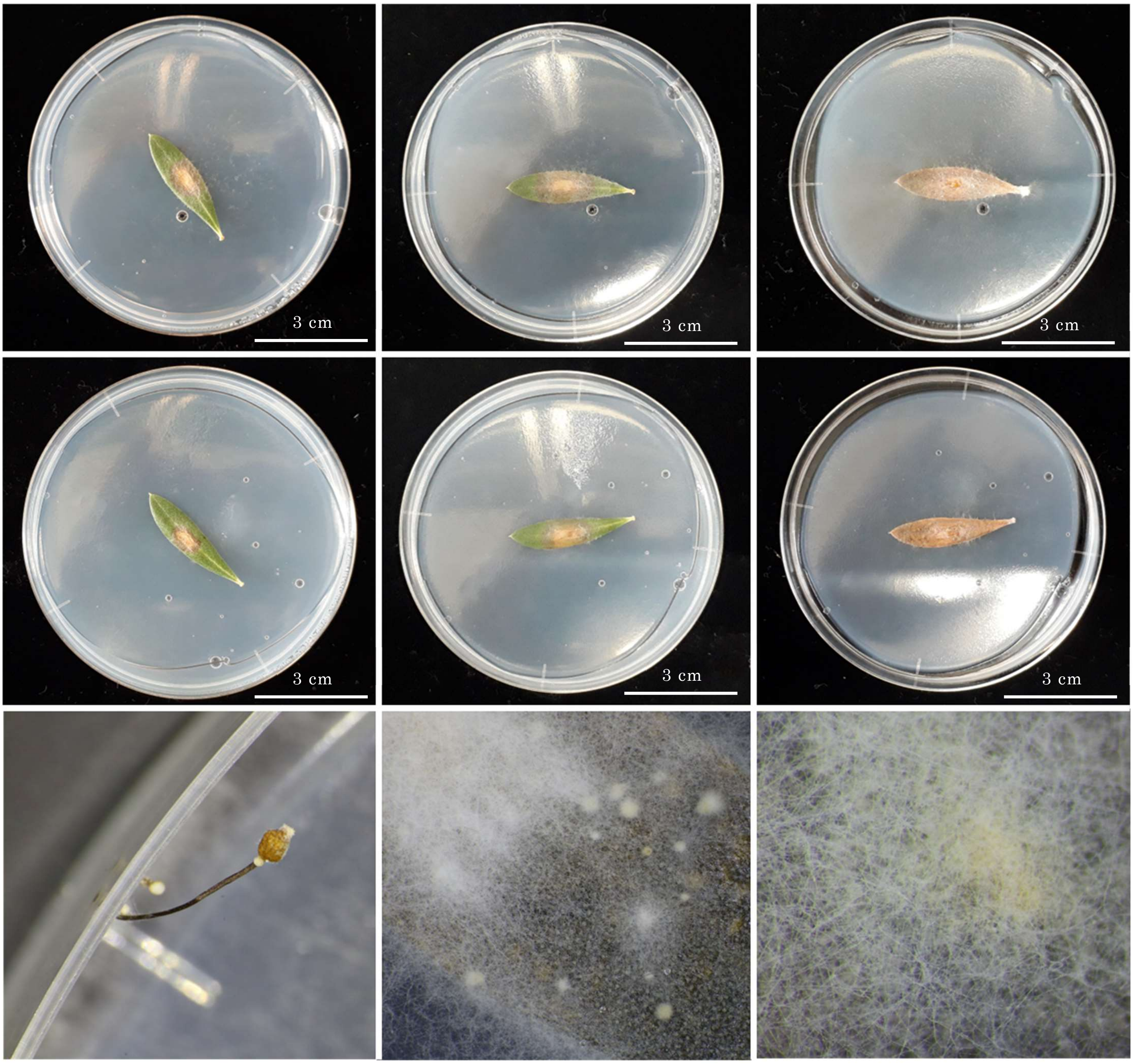

Fig. 10: *Cryptomarasmius ligustrumae* to *O. europaea*. All leaves are injured without surface sterilization. Photos below are enlarged surface and basidiomata. Each leaf is after 12 days, 15 days, 39 days from left.

3.3. Discussion

In the injured leaves of *C. aucubae* to *A. japonica*, *C. hederae* to *H. rhombea*, *C. ligustrumae* to *L. lucidum* and *C. ligustrumae* to *O. europaea*, the dead of leaves and the occurrences of the basidiomata were observed. Since these reactions were not observed in the intact leaves (without two leaves) and the controls, these results suggest that *C. aucubae*, *C. hederae* and *C. ligustrumae* have properties of penetrating to plant bodies from the wounds and causing the plants to die. Moreover, the differences of the results between *C. ligustrumae* to *A. japonica* and *C. ligustrumae* to *L. lucidum* indicated that these reactions do not occur if the *C. ligustrumae* is inoculated to the different plants from its host and it shows the host specificity of *C. ligustrumae*. To compare of the reactions of *Cryptomarasmius* to the plant component , the experiment to add the plant extract from the host of *Cryptomarasmius* to culture medium could be conducted. Moreover, the results of this experiment probably provide the basis to discuss the mechanism of the host specificities of *Cryptomarasmius* because this experiment possibly shows whether the host compositions relate to the formations of the basidiomata of *Cryptomarasmius* or not.

In this study, there were two patterns in the spread of the dead area. one was along the main veins of leaves. The other was gradually. This results suggest that some species of *Cryptomarasmius* spread its hyphae widely along or in the main vein of leaf. In this experiment, the main veins were injured so the hyphae could penetrate to them easily. This suspects that the hyphae of some species of *Cryptomarasmius* grow and spread through the inside of the main vein. To compare how the dead area spread, the additional experiment should be conducted to injure the different parts of leaves.

In two of four injured leaves of *C. ligustrumae* to *O. europaea* and all injured leaves of *C. ligustrumae* to *L. lucidum*, the formations of basidiomata were observed. The basidiomata of *C. ligustrumae* to *O. europaea* formed at the edge of petri dish while those of *C. ligustrumae* to *L. lucidum* formed on the leaves. The reason for the occurrences of the basidiomata at the edge of petri dish is presumed that the environment at the edge of the petri dishes changed more rapidly than inside. Some fungi are known to form their basidiomata at high place to spread their spores widely. Moreover, Hirama et al. (2002) that the stimulations such as temperature and light changes are necessary for some fungi to form and their basidiomata. In many cases, when the specimens of *Cryptomarasmius* form their basidiomata in moist chamber, the growth of their basidiomata smaller and weaker so the external stimulations probably strongly related to the growth of the basidiomata of *Cryptomarasmius*.

Özcan and Matthäus (2017) that *O. europaea* has many polyphenols that have antibacterial properties. However, *C. ligustrum* grow on fallen leaves of *O. europaea* in nature and in this inoculation study, the leaf death and the formation of basidiomata were observed. These suggest that *C. ligustrum* probably have resistance or the ability of decomposition to these antibacterial polyphenols.

Comparing the leaves of *C. hederae* to *H. rhombea* and other leaves, the spreads of dead area of *C. hederae* to *H. rhombea* were smaller than other leaves. This result suggests that the ability of *C hederae* to penetrate and wither plants is weaker than *C. ligustrumae* and *C. aucubae*, or the susceptibility of *H. rhombea* is lower than *A. japonica*, *L. lucidum* and *O. europaea*. *H. rhombea* grows closer to the ground where many fungi exist than *A. japonica*, *L. lucidum* and *O. europaea*, so *H. hederae* probably has stronger resistance to fungi.

In the experiment reported by Otsubo et al. (2011), the hyphae of *C. aucubae* were inoculated to the injured leaves of *A. japonica* and the result was that blotches occurred after eight days and the leaves fell after sixteen days. In the present study, the blotches occurred also after eight days but their area spread overall after forty days. Otsubo et al. (2011) used cut branches for their experiment while only cut leaves were used in this study. In the case of cut branches, vessels of branches send water to leaves so the material movement in veins is more intense than in the case of only leaves. The blotches spread along main veins so the difference of the spread speed is probably caused by the amount of material movement in veins. In inoculation study, the responses of plants are depended on their conditions. In the experiment using cut branches and leaves, the responses often become greater than in nature. The additional experiment that uses cut branches or seedling should be conducted to observe the differences of their responses.

In this study, the information of physiological characteristics of *Cryptomarasmius* are added. The information will contribute to reveal pathogenicity of *Cryptomarasmius*. However, there are also many experiments that should be done. In the future, the author will try these experiment and contribute to reveal physiological characteristics of *Cryptomarasmius*, especially their pathogenicity to various plants.

4. Conclusions

Fungi are very important in nature in that they decompose the remains of animals and plants, and reduce them to inorganic nutrients for plants. Among them, leaf-litter fungi contribute greatly to soil fertility. However, there are few studies of the diversity of these fungi because their basidiomata are often small-sized and they are difficult to find and identify based on morphologies.

Some species of *Cryptomarasmius* have host specificities so these fungi are easier to find and identify than other litter-decomposed fungi that form small-sized basidiomata. Hence, the species of *Cryptomarasmius* are suitable to study their physiological characteristics such as their litter decomposition process.

Moreover, Otsubo (2011) reported that *C. aucubae* has pathogenicity to its host plant, *A. japonica*. This suggests that other species of *Cryptomarasmius* also have pathogenicity to their host plants. In Japan, the known species of *Cryptomarasmius* are only *C. aucubae* that grows on fallen leaves of *A. japonica* (Neda and Doi, 1998) and *Cryptomarasmius* sp. that grow on fallen leaves of *P. tobira* (Kasuya et al. 2024). However, there are more diverse species of *Cryptomarasmius* outside Japan that have host specificities, so the author collected the specimens tentatively treated as the species of *Cryptomarasmius* that grow on various plants other than *A. japonica* and *P. tobira* in Japan. These host plants are widely distributed and cultivated in Japan so it is important for the plant protection and cultivation to reveal the relationships between these specimens and their host plants.

However, these Japanese specimens are different to *C. aucubae* and *Cryptomarasmius* sp. (Kasuya et al., 2024) in their host plants and morphological characteristics. It is necessary to describe and classify the specimens to study their physiological characteristics. For these reasons, in this study the author firstly conducted taxonomic studies of the Japanese specimens and then, conducted inoculation experiment using these fungi.

In taxonomic study, three new species, *C. hederae*, *C. hispidus*, *C. ligustrumae* were described and one species *C. exustoides* were newly recorded in Japan. These species could be distinguished from the Japanese specimens *C. aucubae* and *Cryptomarasmius* sp. on *P. tobira* (Kasuya et al., 2024) by their morphological characteristics and this result was supported by phylogenetic analyses. These specimens can be distinguished mainly in the sizes of basidiomata and basidiospores, and the existence of caulocystidia.

In addition, *C. aucubae*, *C. hederae* and *C. ligustrumae* inoculated to their host plant and the reactions were observed. In the four patterns of injured leaves (*C. aucubae* to *A. japonica*, *C. ligustrumae* to *L. lucidum*, *C. hederae* to *H. rhombea*, *C. ligustrumae* to *O. europaea*), plant death and hyphal growth were observed. In addition, in the three pattern of injured leaves, (*C. ligustrumae* to *L. lucidum*, *C. hederae* to *H. rhombea*, *C. ligustrumae* to *O. europaea*), the formations of basidiomata of the fungal species were observed. This results suggest that some species of *Cryptomarasmius* have the ability to penetrate to plant bodies from wound, cause them to die, decompose their host and form their basidiomata.

By the present study, the knowledge of the taxonomy, phylogeny and physiological characteristics of *Cryptomarasmius* were newly added. However, there are other species of *Cryptomarasmius* that were described based on morphological characteristics only and without any phylogenetic data. Moreover, also regarding physiological characteristics of the genus, there are many experiment that should be conducted additionally. In the future, the author will try to solve these issues raised through in the present study and reveal the detailed physiological characteristics of the species of *Cryptomarasmius*. Such studies could contribute to reveal the physiological characteristics of the litter-decompose fungi that form small-sized basidiomata and have not been studied but important in nature.

5. Acknowledgements

The author gratefully acknowledge Dr. Taiga Kasuya for his supervise in this study and providing specimens, Dr. Hideyuki Nagao for suggestions in the culture experiments, Dr. Kentaro Hosaka for supporting to obtain sequence data, Mr. Shohei Wada for guidance in the microscope observations and providing specimens. The author also thank Dr. Hitoshi Neda for advising on the culture experiments, Dr. Tomotsugu Arikawa for supporting for the use of experimental equipment and identifying the plant species, Dr. Dai Togane for supporting for using experimental equipment, Mr. Atsushi Nagajima for advising on the microscope observations, Ms. Airi Urabe and Ms. Miyu Ii for facilitating the fieldwork.

References

Antonín, V. (2007). Monograph of *Marasmius*, *Gloiocephara*, *Palaeocephala* and *Setulipes* in tropical Africa. Fungal Flora Tropical Africa. 1:1-177.

Antonín, V., Ryoo, R., Ka, K-H. & Shin, H.D. (2012) Marasmioid and gymnopoid fungi of the Republic of Korea. 5. *Marasmius* sect. *Hygrometrici. Mycotaxon* 119: 405–411.

Aron, C. (2020). New and not so new records of *Cryptomarasmius corbariensis* from Anglesey. Field Mycology, 21(3), 84-86.

Bozok, F., Taşkın, H., Büyükalaca, S., Doğan, H. H., & Assyov, B. (2018). *Cryptomarasmius corbariensis* (Physalacriaceae, Agaricales) in Turkey with first molecular data on the species from Eurasia. Nova Hedwigia, 107(1-2), 110-116.

Desjardin, D.E., Horak, E. (1997). *Marasmius* and *Gloiocephala* in the South Pacific region: Papua New Guinea, New Caledonia and New Zealand Taxa 2. Taxonomic monograph of Agaricales II. Bibliotheca Mycologica 168: 84–145.

Dutta, A. K., & Acharya, K. (2018). First record of fungus *Cryptomarasmius* TS Jenkinson & Desjardin (Physalacriaceae: Agaricales: Basidiomycota) from India. Journal of Threatened Taxa, 10(3), 11464-11469.

Edgar, R. C. (2004a). MUSCLE: multiple sequence alignment with high accuracy and high throughput. Nucleic acids research, 32(5), 1792-1797.

Edgar, R. C. (2004b). MUSCLE: a multiple sequence alignment method with reduced time and space complexity. BMC bioinformatics, 5, 1-19.

Fernandez, R. D., Ceballos, S. J., Aragón, R., Malizia, A., Montti, L., Whitworth-Hulse, J. I., ... & Grau, H. R. (2020). A global review of *Ligustrum lucidum* (OLEACEAE) invasion. The Botanical Review, 86, 93-118.

Guindon, S., Dufayard, J. F., Lefort, V., Anisimova, M., Hordijk, W., & Gascuel, O. (2010). New algorithms and methods to estimate maximum-likelihood phylogenies: assessing the performance of PhyML 3.0. Systematic biology, 59(3), 307-321.

Hall, T. A. (1999, January). BioEdit: a user-friendly biological sequence alignment editor and analysis program for Windows 95/98/NT. In Nucleic acids symposium series (Vol. 41, No. 41, pp. 95-98).

Hirama, J., Yanagibashi, H., Matsuda, M., Ishida, R., Miyamoto, N. (2002). Relationship between the bio-electric potential and the morphogenetic properties of *Grifora frondosa* under different light stimuli. IEEJ Transactions on Electronics, Information and Systems, 122 (9), 1679-1685.

Hoang, D. T., Chernomor, O., Von Haeseler, A., Minh, B. Q., & UFBoot, L. V. Improving the ultrafast bootstrap approximation., 2018, 35. DOI: https://doi.org/10.1093/molbev/msx281, 518-522.

Hosaka, K. (2009). Phylogeography of the genus *Pisolithus* revisited with some additional taxa from New Caledonia and Japan. Bull Nat Mus Nat Sci Ser B 35: 151-167

Hosaka, K., Castellano, MA. (2008). Molecular phylogenetics of *Geastrales* with special emphasis on the position of *Sclerogaster*. Bulletin of the National Museum of Nature and Science, Series B 34(4): 161-173

Hosaka, K., Kasuya, T., Reynolds, H. T., & Sung, G. H. (2010). A new record of *Elaphomyces guangdongensis* (Elaphomycetaceae, Eurotiales, Fungi) from

Taiwan. Bulletin of the National Museum of Natural Science, serie B, 36, 107-115.

Jenkinson, T. S., Perry, B. A., Schaefer, R. E., & Desjardin, D. E. (2014). *Cryptomarasmius* gen. nov. established in the Physalacriaceae to accommodate members of *Marasmius* section *Hygrometrici*. Mycologia, 106(1), 86-94.

Kaplan, D., Uzun, Y., & Kaya, A. (2021). A new record for the Physalacriaceae family in Turkey. Anatolian Journal of Botany, 5(2), 120-123.

Kasuya, T., Nakajima, A., Wada, S., Ito, E., Urabe, A., Hosaka, K. (2024). An undescribed species of the genus *Cryptomarasmius* growing on leaf litter of *Pittosporum tobira*. Abstracts of Papers Presented at the 68th Annual Meeting of the Mycological Society of Japan (p. 60). The Mycological Society of Japan.

Kiyashko, A. A., Malysheva, E. F., Antonin, V., Svetasheva, T. Y., & Bulakh, E. M. (2014). Fungi of the Russian Far East 2. New species and new records of *Marasmius* and *Cryptomarasmius* (Basidiomycota). Phytotaxa, 186(1), 1-28.

Kühner, R. (1933). Etudes sur le genre *Marasmius*. Botaniste 25:57-115.

Neda, H. & Doi, Y. (1998) Notes on Agarics in Kyushu District. Memoirs of the National Science Museum 31: 89–95

LI, S., & BAU, T. (2024). New findings of *Cryptomarasmius* (Physalacriaceae, Agaricales) from Jilin Province, China. Phytotaxa, 641(1), 57-65.

Minh, B. Q., Schmidt, H. A., Chernomor, O., Schrempf, D., Woodhams, M. D., Von Haeseler, A., & Lanfear, R. (2020). IQ-TREE 2: new models and efficient methods for phylogenetic inference in the genomic era. Molecular biology and evolution, 37(5), 1530-1534.

Murata, H. (2014). APG Standard Makino's Illustrated Flora I. (Hokuryukan)

Nylander, J. A. A. (2004). MrModeltest. Version 2. Program distributed by the author. Uppsala University. Evolutionary Biology Centre, Uppsala. Available from https://github. com/nylander/MrModeltest2 [accessed 16 Sep. 2020].

Onishi, S. (2010). PhotoRuler version 1.1.3. https://www.inocybe.info/_userdata/ruler/PhotoRuler.html.

Osono, T. (2018). Basic Fungal Ecology. (Kyoritsu Shuppan)

Otubo, K., Akahori, C., Harada, Y. (2011). Pathogenicity of *Marasmius aucubae*; the litter decomposing basidiomycete for *Aucuba japonica*. Abstracts of Papers Presented at the 55th Annual Meeting of the Mycological Society of Japan (p. 100). The Mycological Society of Japan.

Özcan, M. M., & Matthäus, B. (2017). A review: Benefit and bioactive properties of olive (*Olea europaea* L.) leaves. European Food Research and Technology, 243, 89-99.

Puccinelli, C., Capelari, M. (2009). *Marasmius* do Parque Estadual das Fontes do Ipiranga, São Paulo, SP, Brasil: Seções Globulares, Hygrometrici, Marasmius e Neosessiles. Hoehnea 36(2): 249-258.

Ronquist, F., Teslenko, M., Van Der Mark, P., Ayres, D. L., Darling, A., Höhna, S., ... & Huelsenbeck, J. P. (2012). MrBayes 3.2: efficient Bayesian phylogenetic inference and model choice across a large model space. Systematic biology, 61(3), 539-542.

Singer, R. (1976). Marasmieae (Basidiomycetes Tricholomataceae) monograph no. 17, Flora Neotropica. The New York Botanical Garden, New York: 1-348.

Singer, R. (1989). New taxa and new combinations of Agaricales (Diagnoses fungorum novorum Agaricalium IV). Fieldiana (Botany, New Ser) 21:1-133.

Swofford, DL. (2002). PAUP*: phylogenetic analysis using parsimony and other methods (*PAUP version 4.0 beta 10). Sinauer, Sunderland.

Tan, YS., Desjardin, DE., Perry, BA., Vikineswary, S., Noorlidah, A. (2009). *Marasmius* sensu stricto in peninsular Malaysia. Fungal Divers 37:9V100.

Vilgalys, R., & Hester, M. (1990). Rapid genetic identification and mapping of enzymatically amplified ribosomal DNA from several *Cryptococcus* species. Journal of bacteriology, 172(8), 4238-4246.

White, T. J., Bruns, T., Lee, S. J. W. T., & Taylor, J. (1990). Amplification and direct sequencing of fungal ribosomal RNA genes for phylogenetics. PCR protocols: a guide to methods and applications, 18(1), 315-322.

↓論文印刷前に、下の行を選択して右クリック「フィールドの更新」すること↓

- 本文 35 字×25 行×70 ページ、全 12427 words